Cell Host & Microbe

Changes in Microbiome Confer Multigenerational Host Resistance after Sub-toxic Pesticide Exposure

Graphical Abstract

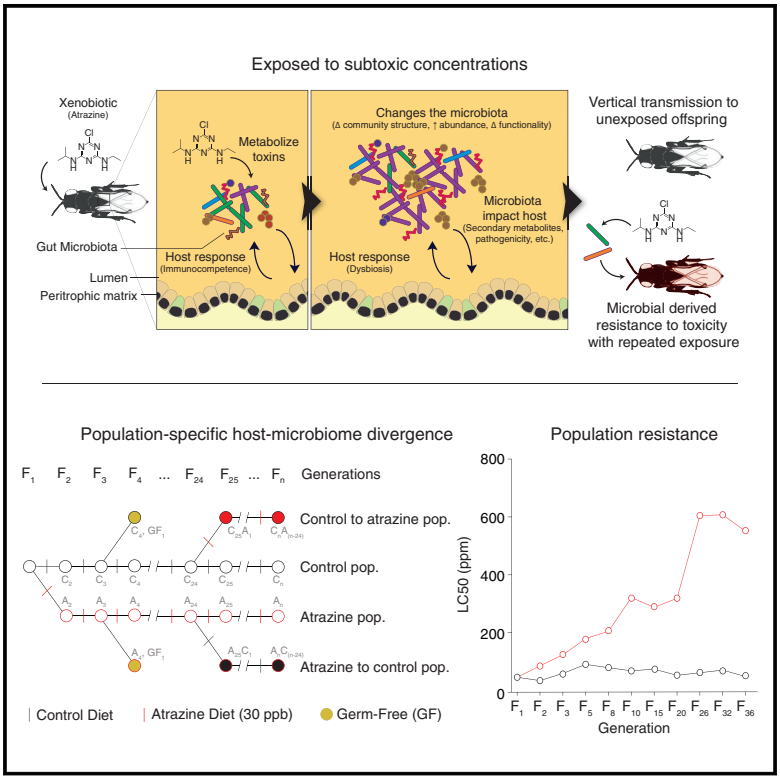

Highlights

- Atrazine exposure leads to changes in host microbiota that are vertically transmitted
- Atrazine is toxic to the hymenopteran model *Nasonia* at very high doses
- Specific gut bacteria metabolize atrazine and are enriched after atrazine exposure
- Multi-generational exposure causes host genome divergence

Authors

Guan-Hong Wang, Brittany M. Berdy, Olivia Velasquez, Nikola Jovanovic, Saleh Alkhalifa, Kevin P.C. Minbiole, Robert M. Brucker

Correspondence

brucker@rowland.harvard.edu

In Brief

Wang et al. demonstrate low-level toxicity of atrazine in *Nasonia* wasps. A single, sub-toxic exposure causes changes in the gut microbiota that are transmitted to the next generation. Populations that are exposed every generation become resistant to high-level exposure, with atrazine resistance conferred by metabolic capabilities of at least two rare bacteria.

Wang et al., 2020, Cell Host & Microbe *27*, 1–12
February 12, 2020
https://doi.org/10.1016/j.chom.2020.01.009

CellPress

Please cite this article in press as: Wang et al., Changes in Microbiome Confer Multigenerational Host Resistance after Sub-toxic Pesticide Exposure, Cell Host & Microbe (2020), https://doi.org/10.1016/j.chom.2020.01.009

Cell Host & Microbe
Article

Changes in Microbiome Confer Multigenerational Host Resistance after Sub-toxic Pesticide Exposure

Guan-Hong Wang,[1] Brittany M. Berdy,[1] Olivia Velasquez,[1] Nikola Jovanovic,[1] Saleh Alkhalifa,[2] Kevin P.C. Minbiole,[2] and Robert M. Brucker[1,3,*]
[1]Rowland Institute at Harvard University, Cambridge, MA 02142, USA
[2]Department of Chemistry, Villanova University, Villanova, PA 19085, USA
[3]Lead Contact
*Correspondence: brucker@rowland.harvard.edu
https://doi.org/10.1016/j.chom.2020.01.009

SUMMARY

The gut is a first point of contact with ingested xenobiotics, where chemicals are metabolized directly by the host or microbiota. Atrazine is a widely used pesticide, but the role of the microbiome metabolism of this xenobiotic and the impact on host responses is unclear. We exposed successive generations of the wasp *Nasonia vitripennis* to subtoxic levels of atrazine and observed changes in the structure and function of the gut microbiome that conveyed atrazine resistance. This microbiome-mediated resistance was maternally inherited and increased over successive generations, while also heightening the rate of host genome selection. The rare gut bacteria *Serratia marcescens* and *Pseudomonas protegens* contributed to atrazine metabolism. Both of these bacteria contain genes that are linked to atrazine degradation and were sufficient to confer resistance in experimental wasp populations. Thus, pesticide exposure causes functional, inherited changes in the microbiome that should be considered when assessing xenobiotic exposure and as potential countermeasures to toxicity.

INTRODUCTION

Agrochemicals used to fertilize crops and control pest species pose one of the greatest xenobiotic exposure risks to many organisms, including humans. The herbicide atrazine is the second-most-sold pesticide globally (Baker and Stone, 2015). The United States Environmental Protection Agency has deemed that the continuous daily average of 3 parts per billion (ppb) of atrazine, a broad leaf herbicide, in fresh and potable water is acceptable; and it has been detected in 78% of drinking water throughout the U.S. (Mannix, 2016). Previous studies have shown atrazine has multiple impacts on a host animal, including changes in stress response gene expression (Le Goff et al., 2006), protein production (Thornton et al., 2010), male mating ability (Vogel et al., 2015), egg production (Badejo and Vanstraalen, 1992), mating choice (McCallum et al., 2013), mitochondrial dysfunction, insulin resistance (Lim et al., 2009), and overall survival (Rohr et al., 2006). While it is generally thought that animals lack the pathways to metabolize the pesticide, naturally occurring bacteria in the soil and water have the capability of metabolizing atrazine into secondary compounds such as cyanuric acid, biuret, and allophanate and using them as carbon and nitrogen sources (Bellini et al., 2014). All animals have symbiotic microbes in their guts that perform a variety of beneficial roles such as aiding in digestion (Douglas, 2015). However, little is known about how environmental xenobiotic chemicals like atrazine change the gut microbiome and the heritable fitness effects of the host-microbe phenotypes.

When xenobiotics are ingested, these chemicals can either be absorbed directly by the host or metabolized by gut microbiota. In the latter case, the toxicity of xenobiotics can be enhanced (Bellini et al., 2014; Dierickx, 1999) or mitigated (Kikuchi et al., 2012) through metabolic pathways of the microbes. In this study, we examine the impact of acute or continuous subtoxic pesticide exposure to the model wasp species *Nasonia vitripennis* across 36 non-overlapping generations to determine (1) whether acute subtoxic exposure results in inherited alterations to the gut microbiome, (2) whether long-term subtoxic exposure perturbs the functions of this community, (3) whether this change impacts host fitness, and (4) whether phylosymbiosis—the observation that microbiota are congruent with host-species divergence—can be experimentally observed in response to changing microbiome function and host adaptation.

To obtain a better understanding of the host-microbe interactions associated with xenobiotic exposure and its impact across generations, we performed multi-omics analyses on experimental populations of the hymenopteran insect model, *Nasonia*. *Nasonia* is an ideal genetics model for laboratory experiments in Hymenoptera due to its simple husbandry, known developmental successions of microbiome, ability to generate gnotobiotic/germ-free (GF) reproductive adults, the global range of natural populations, and short—non-overlapping—generations (Brucker and Bordenstein, 2013; Werren et al., 2010). Following an acute exposure to atrazine (300 ppb) within a generation, we observed a shift in the dominant members of the microbiome of the host that was also inherited in subsequent, unexposed generations. Considering that *Nasonia* maternally receives its species-specific microbial community (Brucker and Bordenstein, 2013), the observations described here indicate the inability of these populations to return to the ancestral-like microbiome post-atrazine exposure due to losses of the microbial reservoir or other heritable effects changing the host-microbe regulatory mechanisms. We also observed shifts in microbial abundance and diversity across generations whose foundresses were

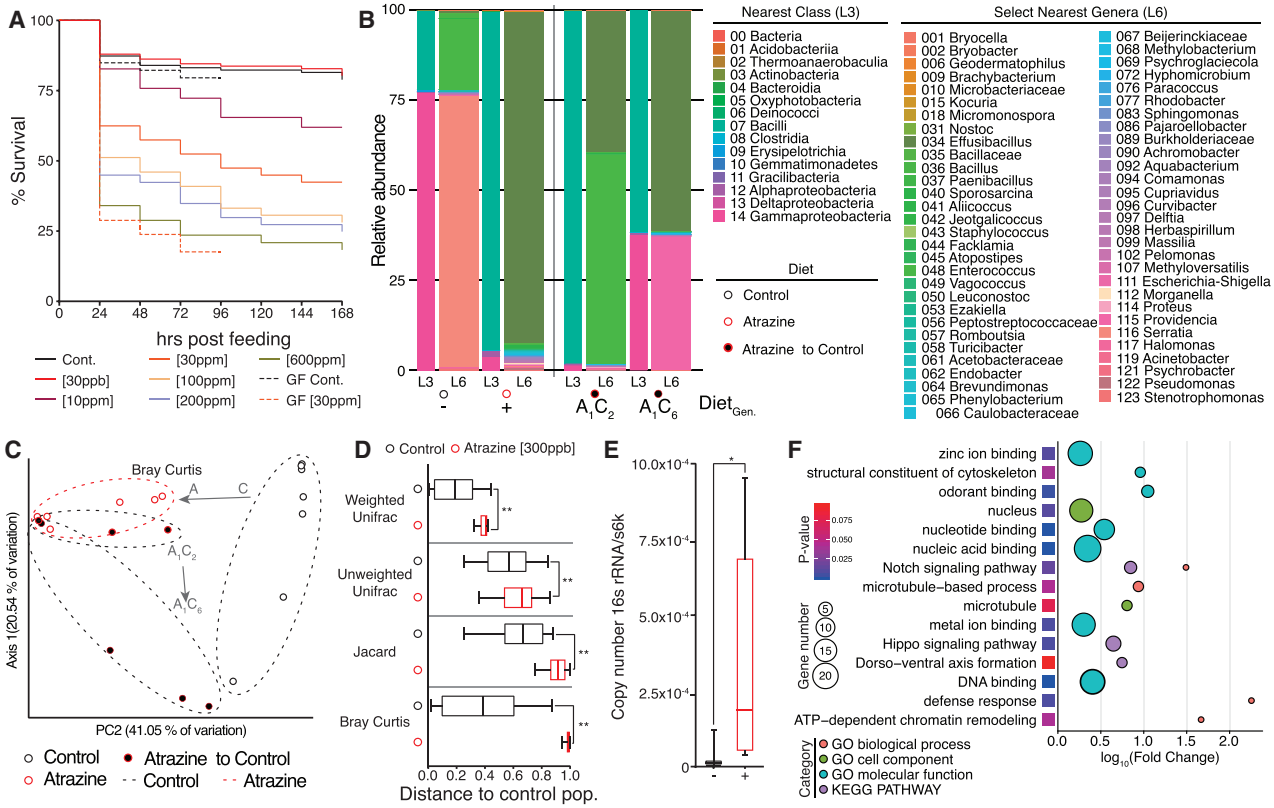

Figure 1. Impact of Atrazine Exposure on *N. vitripennis*

(A) Survivorship of *N. vitripennis* following atrazine exposure. For conventional rearing wasps, there was significantly increased ($p < 0.0001$) mortality with $\geq$ 30 ppm atrazine exposure compared to control. There was a significant increase in mortality for the atrazine exposed GF compared to conventional reared wasps exposed to 30 ppm atrazine ($p < 0.0001$). Survival curves were generated using GraphPad Prism 7.01 (Log-rank test).

(B) The composition of gut bacterial constituents at nearest class (L3) and nearest genus (L6) levels (n = 7, 10, 4, 5 for control, atrazine, A_1C_2, A_1C_6, respectively). Replicates are grouped via mean-ceiling.

(C) Principal coordinate analysis (PCoA) score plot using QIIME 2 software and Bray-Curtis analysis.

(D) Gut microbiota intra- and inter-group variations of control diet and atrazine diet populations. **$p < 0.01$; PERMANOVA test.

(E) Total microbiome density increased 96 h after atrazine exposure compared to the control (total bacterial *16S* rRNA gene copies relative to *N. vitripennis* single copy gene *S6K* using qPCR). Box-and-whisker plots show max, min, and median values, respectively. **$p < 0.01$; Mann-Whitney U test.

(F) Go and KEGG enrichment analysis of transcriptomes between control and atrazine exposure. The second-level GO terms were shown in the plot and enrichment analysis was performed using functional annotation tool DAVID.

exposed to atrazine (30 ppb), ultimately resulting an increase in host tolerance to atrazine beyond the first generation's natural tolerance. These tolerances were maintained for more than 10 generations in a subsequent atrazine-unexposed population, which was split from the atrazine-exposed population, indicating that the derived benefit from the shifted microbiome-host association is transmitted from one generation to the next. In addition, when rearing wasps GF, we observed a more than 10-fold decrease in resistance to the pesticide.

RESULTS

Multi-omics Analysis Reveals Changes in Microbiome Structure and Host Physiology after Acute Exposure to Xenobiotics

We first exposed a naive laboratory line of *N. vitripennis* (strain AsymCx) to assess the baseline toxicity of atrazine. We observed a significant decrease in survival in a dose-dependent manner with a lethal concentration of 50% of the population (LC_{50}) at 45.50 ± 15.73 parts per million (ppm) (Figure 1A). When reared GF, we observed a significant decrease in survival compared to conventionally reared wasps receiving the low-concentration atrazine-sucrose diet (atrazine diet) (30 ppm), but not with control-sucrose diet (control diet) (Figure 1A). This result suggests the importance of the microbiota in detoxifying atrazine. We used targeted amplicon sequencing of the *16S* rRNA gene to assess changes in the abundance and composition of the gut microbiome following acute exposure to atrazine (Figure S1A) in a subset of the first generation that was exposed to 300 ppb—similar to that encountered by pollinators in newly sprayed agricultural fields and streams (Baker and Stone, 2015). The population receiving the atrazine diet had a significantly different bacterial community structure than the control population fed the control diet (Figures 1B–1D). In the atrazine-exposed population, we observed a significant increase in the abundance of the recently described Firmicute, *Effusibacillus* (Watanabe

et al., 2014) (Figure 1B). The closest known relatives of *Effusibacillus* are extremophiles, and little else is known about this genus. This phylum shift toward Firmicutes is similar to that observed in water and soil microbial communities that are exposed to atrazine (Bellini et al., 2014) as well as in the guts of diseased frogs (Knutie et al., 2018). Wasps in the atrazine-exposed treatment had a more diverse microbiome than did wasps in the control treatment using the Shannon index. However, while there was a change in species richness (Figure S1B), there were no changes in species evenness (Figure S1C). Using quantitative PCR (qPCR), the total microbial load of *N. vitripennis* (*16S* copy number/*S6K* copy number) significantly increased 96 h after 300 ppb atrazine feeding (Figure 1E, $p < 0.05$, Mann-Whitney U test, primers listed in Table S1). This result indicates that even a single exposure to only 300 ppb of the herbicide results in an increase of overall bacterial load in the host, which could be accounted for by change in abundance of several taxa despite the presence of similar operational taxonomic units (OTUs) across the populations. Furthermore, when we switched the offspring of the atrazine-exposed population to the control diet for six generations (Figure S1A), we observed that the bacterial microbiome remained most similar to that of the atrazine-exposed parent (Figures 1B, 1C, and S1D–S1G). This result indicates that the disruption to the microbiome after acute exposure to atrazine is inherited across generations even after exposure is removed. Using total RNA-seq from exposed and naive populations of *Nasonia*, we detected constitutively active bacteria of the microbiome that differed from the *16S* analysis, including multiple atrazine metabolizing genes of bacterial origin across both control or atrazine diet samples (Figure S1H and Table S2). The differences between the populations indicated that the active bacteria are commonly shared between populations, with some exceptions: the *Serratia* and *Pseudomonas* species were more active in the atrazine-exposed populations, and the genus *Clostridium* was significantly underrepresented in the atrazine-exposed population (Figure S1H).

We assessed the impact of atrazine on the host physiology by comparing the transcriptome and proteome of wasps unexposed to atrazine and wasps exposed to 300 ppb of atrazine. Using transcriptomics, we found 370 differentially expressed genes (out of 13,550) (Figures 1F, S1I, and Table S3), 28 of which were downregulated and 342 were upregulated (Figure S1I). Gene ontology and functional classification showed that the most downregulated genes are involved in immunity and odorant binding, suggesting that atrazine exposure may alter *N. vitripennis* immune function and behavior. Earlier studies in rats (Rooney et al., 2003) and frogs (Brodkin et al., 2007) similarly demonstrated that a single exposure to atrazine can act as an immune disruptor and even affect behavior in mice (Belloni et al., 2011). Most upregulated genes are associated with energy, nucleic acid binding, and metal ion binding pathways (Figure 1F). The upregulation of energy-associated genes upon atrazine exposure suggests that the herbicide may affect mitochondrial function in *N. vitripennis*, which has been previously reported in other systems (Horzmann et al., 2018; Thornton et al., 2010). Genes from three KEGG pathways were also found to be upregulated: Hippo signaling, Notch signaling, and Dorsoventral axis formation (Figure 1F). There is evidence that microbiota can mediate the Notch pathway through innate immune signaling (Troll et al., 2018), which supports the idea that atrazine exposure may affect the microbiota in *N. vitripennis*. The transcripts of cytochrome P450 genes, which function to metabolize potentially toxic compounds in animals, were found to be differentially affected by atrazine exposure. Cytochrome P450 4C1 was significantly upregulated while cytochrome P450 6a14 was significantly downregulated (Table S4). Interestingly, cytochromes as a gene family for detoxification were not significantly enriched (Figure 1F), suggesting *N. vitripennis* lacks an efficient antioxidative response to atrazine exposure. Detoxification enzymes such as cytochrome P450s and glutathione S-transferases (GST) genes in *Drosophila melanogaster* have been reported to be upregulated after atrazine exposure (Le Goff et al., 2006).

Using proteomics, we observed that 27 proteins (out of 1,340) that were differentially expressed after an acute exposure to atrazine (Figure S1J), 10 of which were downregulated (fold change < 0.83, $p < 0.05$) and 17 of which were upregulated (fold change > 1.2, $p < 0.05$) (Table S5). Of the 10 downregulated proteins, two were immunity related, which indicates that atrazine exposure may alter the immune function of *N. vitripennis* (Table S5). While a number of detoxification enzymes were detected using proteomics (4 cytochrome P450s, 16 GSTs, and 1 carboxylesterase) (Table S5), we found no significant difference in expression of these proteins in atrazine-exposed populations. Similar studies in *Apis mellifera* (Al Naggar et al., 2015) have also reported no difference of detoxification enzymes following atrazine exposure, although we do see a difference in expression using RNA-seq—as previously discussed. In this study, we found that 6 out of 17 proteins associated with energy production were upregulated in response to atrazine (Table S5), paralleling the RNA-seq results above. These results suggest that exposure to atrazine may affect mitochondrial function in *N. vitripennis*, as well. Taken together, the RNA-seq and proteomics results indicate that the host is not responding significantly to atrazine exposure through predicted detoxification pathways but does exhibit a response through immunity pathway genes, which are associated to the disrupted microbiota and are significantly responsive.

Multigenerational Sub-toxic Exposure to Atrazine Impacts Tolerance to Xenobiotics

To further investigate how these inherited changes to the gut microbiome impact host fitness, we maintained the concurrent atrazine-exposed and control populations for over 36 generations by feeding a subtoxic concentration of atrazine diet (30 ppb) or control diet, respectively (Figure 2A). Through successive generations, the control population maintained an average LC_{50} of 67.68 ± 4.99 ppm, while the atrazine-exposed population exhibited an increase in tolerance. By the eighth generation, we observed a nearly 3-fold higher tolerance in the atrazine-exposed population (A_8 211.95 ppm, 95% CI 122.91-440.48) compared to the control (C_8 84.52 ppm, 95% CI 39.86-261.39). By the 36th generation, the atrazine-exposed population had an LC_{50} about 10 times higher than the control (A_{36} 561.55 ppm 95% CI 312.22-1060.70; C_{36} 53.94 ppm 95% CI 25.74-106.62) (Figure 2B). After 36 generations, the atrazine-exposed population also demonstrated higher tolerance to the herbicide glyphosate compared with the control population, but there

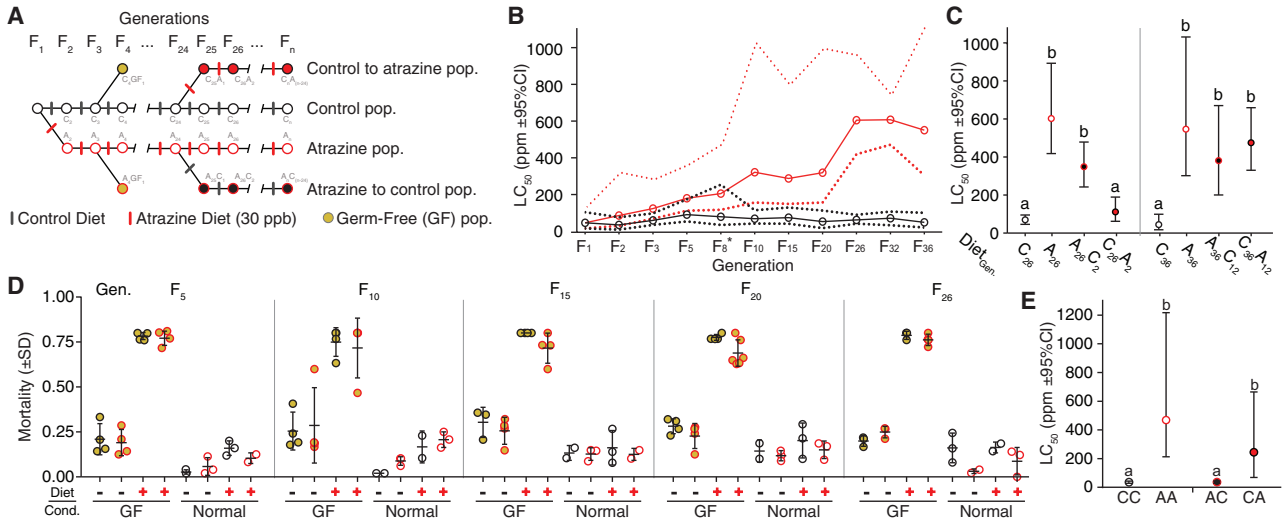

Figure 2. Atrazine-Exposed Population Shows Increasing Tolerance to Atrazine and the Tolerance Is Inheritable

(A) Populations of n = 50 female founders and n = 15 males/generation fed on a control diet (black), or an atrazine diet (red), for 36 generations (F_{36}). At the 25th generation, populations were split to establish new populations with switched diets populations (red with back infill for atrazine population switched to control diet and black with red infill for control population switched to atrazine diet). For certain generations, we also rear them in germ-free media.

(B) The LC_{50} increased across generations in the atrazine-exposed population while remaining constant in the control population. All generations from F_8 onward were significantly different between atrazine-exposed and control populations.

(C) Comparing LC_{50} for the offspring of each populations' 25th and 35th generations. Tolerance is inherited in the atrazine-exposed population after switching to the control diet. It shows convergent atrazine resistance in the control population after switching to the atrazine diet.

(D) Proportion of dead adult *Nasonia*, either germ-free or conventionally raised on fly pupae (Cond.) recorded after 96 h of feeding either a control sucrose diet (black "-") or 3 ppm atrazine sucrose diet (red "+") ($p > 0.05$, Student's t test). The LC_{50} was calculated using Polo Plus-PC software and the plot represents the mean and the 95% level of CI (dashed lines). There was no significant difference in mortality rate with 0 and 3 ppm atrazine diet between the atrazine-exposed and control populations under one generation GF rearing.

(E) The LC_{50} after whole microbiome communities are inoculated into germ-free populations. The LC_{50} was calculated Germ-Free L4 larvae with microbiomes from their con-specific population (atrazine-exposed - red open circle versus control – black open circle) or hetero-specific populations' microbiome (control population that receives the atrazine-exposed population microbiome – CA, black with red circle versus the atrazine-exposed population that receives the control population microbiome – AC, red with black circle) * and letters indicate the resistance ratio calculated by 95%. CI does not include 1.0.

was no difference observed in the tolerance to the insecticide imidacloprid (Figure S2). The observation of glyphosate resistance suggests that the derived microbial community could have protective effects when the host is exposed to other xenobiotics, despite no prior exposure to the compounds.

To assess the stability of the microbiome shift once atrazine exposure was removed, both the atrazine-exposed and control populations were split into sub-lineages after 25 generations and their diets were switched to a conspecific atrazine exposure (Figure 2A). Toxicity was assessed in the offspring from the diet-switched populations, as well as the original lineages, to assess the impact of diet and heritability on the microbiome and herbicide tolerance of the host. Tolerance was still observed after the atrazine-exposed population was switched to a control diet, which was sustained through the 36th generation (Figure 2C). The LC_{50} of the atrazine-to-control diet population was slightly lower than the parental population that had continued exposure to atrazine; however, it remained significantly higher than the control, indicating the inherited microbiome enriched in bacterial species known to detoxify atrazine may be contributing to this tolerance. Once the control population switched to an atrazine diet, we observed a significant increase in tolerance to atrazine compared with the control population after 12 generations (Figure 2C). This pattern is similar to the control and atrazine-exposed populations (Figure 2B) and suggests the atrazine-sucrose diet changed the microbiota and the associated host's response to atrazine. Taken together, these results support the conclusions that atrazine exposure can shift the host microbiome, the shifted microbiome is inherited, and the altered microbiome is unlikely to revert to an ancestral-like microbial community. Stability of the microbiome is likely due to an absent environmental reservoir of the ancestral microbial community or the absence of a selective cost of maintaining the new community.

To determine if this increased tolerance was directly linked to the microbiome, we assessed the mortality rate across generations of *N. vitripennis* from both control and atrazine-exposed populations maintained under GF. We found that both the GF atrazine-exposed and control populations had more than 50% mortality rate when exposed to 3 ppm atrazine (Figure 2D). Furthermore, when we exposed GF L4 larvae with microbiomes from their con-specific population (atrazine-exposed versus control), the control population that receives the atrazine-exposed population microbiome (CA) is significantly resistant to atrazine than the atrazine-exposed population that receives the control population microbiome (AC). It does appear however, that the CA population is less resistant to atrazine than atrazine population fed the atrazine microbiome (AA) (Figure 2E). These

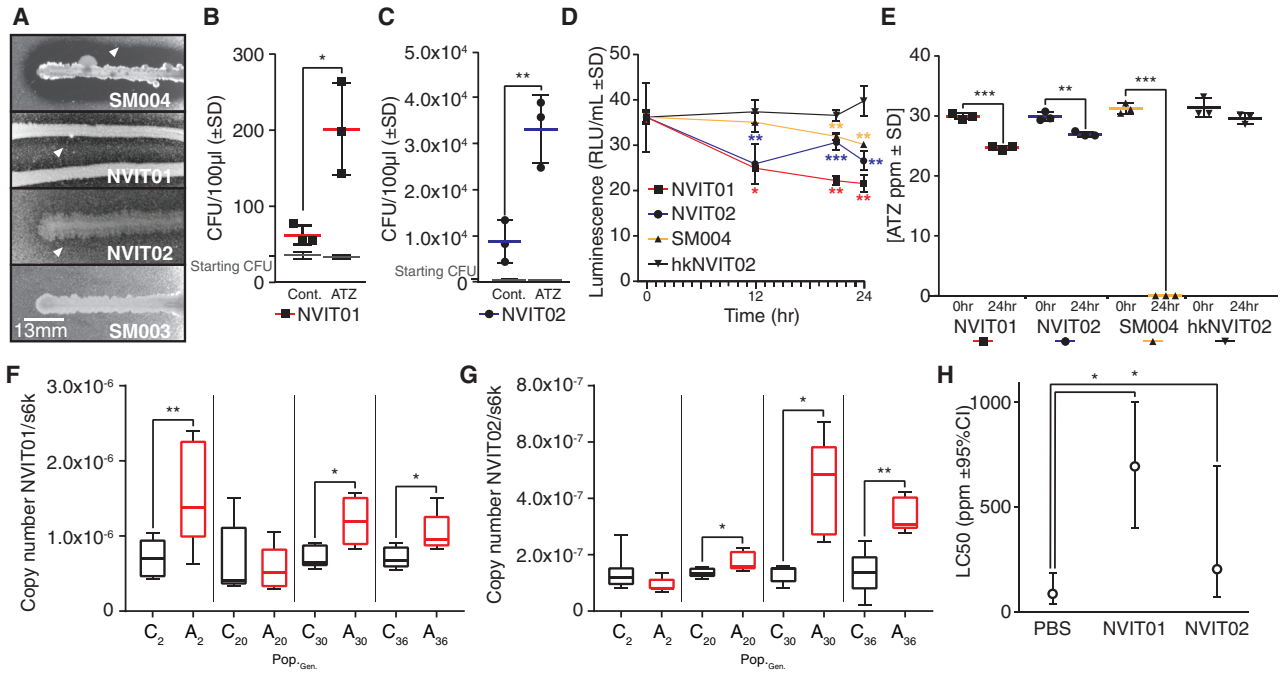

Figure 3. Bacteria Isolated from *N. vitripennis* Can Metabolize Atrazine *In Vivo* and *In Vitro*

(A) Zones of clearing by atrazine-degrading strains isolated from *N. vitripennis* on an atrazine-containing LB agar plate.

(B and C) Colony forming units (CFU) of *S. marcescens* NVIT01 (NVIT01) (B) and *P. protegens* NVIT02 (NVIT02) (C) cultured in MSM and AMSM (30 ppb). The bacterial culture was diluted for plating at 0 and 48 h (B) and 72 h (C) (Student's t test).

(D–F) Bacterial bioluminescence (D) and HPLC (E) assay confirming degradation of atrazine. SM004 is as a positive and heat-killed NVIT02 (hkNVIT02) as a negative control. NVIT01 density (F) (*S. marcescens 16S* rRNA gene copy relative to *N. vitripennis* single copy gene *S6K* using qPCR) and NVIT02 density.

(G) (*P. protegens gyrB* gene copy relative to *S6K* using qPCR) increased in the atrazine-exposed population. Box-and-whisker plots show max, min, and median values, (Mann-Whitney U test).

(H) Comparing LC50 for the first generation offspring's exposure to NVIT01, NVIT02, and control populations. The LC50 was calculated using Polo Plus-PC software and the plot represents the mean and the 95% level of CI. *indicates the resistance ratio calculated by 95% CI and does not include 1.0. *$p < 0.05$, **$p < 0.01$, ***$p < 0.001$.

results strongly indicate that the increased tolerance in the atrazine-exposed population is related to a shifted microbial community or specific microbial members, as opposed to the host detoxication enzymes from above RNA-seq and proteomics analyses. The shift in the microbial community following continuous atrazine exposure may be providing host resistance via detoxification, representing a rapid route of ecological adaptation for the host to cope with novel toxic challenges.

Atrazine-Degrading Bacteria Are Enriched in the Gut of Atrazine-Exposed Population

We used mineral salt media (MSM) that is nitrogen limited to identify bacteria strains from wasp that can respond to the atrazine resistance we observed above. Two strains (NVIT01 and NVIT02) demonstrated zones of clearing, indicating the ability of the bacteria to metabolize high concentrations of atrazine in a solid matrix (Figure 3A). These two strains also showed superior growth on AMSM (containing 30 ppb atrazine) compared to MSM (Figures 3B and 3C), suggesting they can use atrazine as their nitrogen resource. The metabolism of atrazine was verified using a bioluminescence assay that quantifies the concentration of atrazine and/or cyanuric acid (Hua et al., 2015), which decreased in cultures containing NVIT01 and NVIT02 - same as positive control *E. coli* SM004, which is a strain created to degrade atrazine (Hua et al., 2015) while no decrease in negative control heat-killed NVIT02 (hkNVIT02) (Figure 3D). Metabolism of atrazine by these strains was further confirmed using HPLC to quantify atrazine concentrations in nutrition broth media where both NVIT01 and NVIT02 had depleted 20% and 10%, *E. coli* SM004 and hkNVIT02 had depleted 100% and 0%, respectively, of atrazine in the media (Figure 3E).

Given that the atrazine-exposed population had a higher tolerance to atrazine compared to the control, we hypothesized that these two atrazine-degrading isolates (*Serratia marcescens* NVIT01 and *Pseudomonas protegens* NVIT02) would have a higher bacterial density in the atrazine fed population. Using qPCR to quantify bacterial density, we found that the densities of *S. marcescens* NVIT01 (*16S* copy number) and *P. protegens* NVIT02 (*gyrB* copy number) relative to *N. vitripennis* (*S6K* copy number) in the atrazine-exposed population was significantly increased compared with control population (Figures 3F and 3G, * $p < 0.05$, ** $p < 0.01$, Mann-Whitney U test).

S. marcescens NVIT01 and *P. protegens* NVIT02 Confer Atrazine Resistance to Their Host

To determine if the atrazine-degrading microbes, *S. marcescens* NVIT01 and *P. protegens* NVIT02, could confer atrazine resistance to the host, we fed *N. vitripennis* adults from control diet

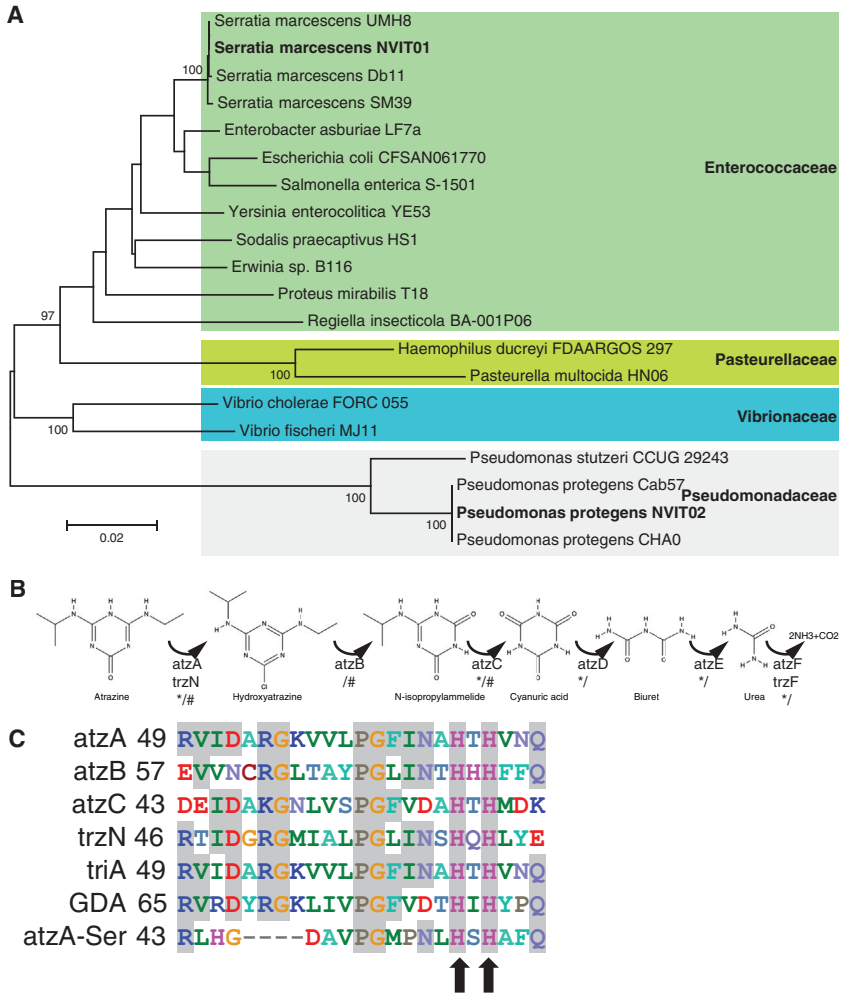

Figure 4. *S. marcescens* NVIT01 and *P. protegens* NVIT02 Comparative Genome Analysis

(A) Phylogenetic tree demonstrating the relationship of *S. marcescens* NVIT01 and *P. protegens* NVIT02 to other closely related bacteria on the basis of *16S* rRNA sequences.

(B) The atrazine metabolizing pathway and the atrazine genes found in *S. marcescens* NVIT01 (*) and *P. protegens* NVIT02 (#).

(C) Alignment of atzA (*Pseudomonas* sp. ADP; AAK50270.1), atzB (*Pseudomonas* sp. ADP; AAC45138.1), atzC (*Pseudomonas* sp. ADP; AAB96621.1); trzN (*Nocardioides* sp. C190; AAL39016.1); triA (*Acidovorax citrulli*; AAG41202.1); GDA (*Escherichia coli* str. K-12; AAC75921.1); atzA-Ser from *S. marcescens* NVIT01. The amino acids were numbered from the N terminus of each protein, and arrows indicate HXH motif region.

population with each of the microbes in sugar solution or PBS in sugar solution as a control. After feeding microbes for one generation, we observed significant resistance to atrazine compared with sugar feeding only (Figure 3H). These results indicate that both *S. marcescens* NVIT01 and *P. protegens* NVIT02 confer atrazine resistance to *N. vitripennis*. Our data also suggest that *S. marcescens* NVIT01 may be pathogenic when at higher loads in the host, which could be a selective pressure to maintain a host-microbe regulatory mechanism (Figure S3). This is not uncharacteristic for this species of bacteria, as *S. marcescens* is known to be an opportunistic pathogen to other animals such as honeybees (Motta et al., 2018). Therefore, it is possible that the *S. marcescens* NVIT01 population densities became too high in *N. vitripennis*, disrupting the host-microbiome resulting in mortality.

Atrazine-Degrading Pathways in *S. marcescens* NVIT01 and *P. protegens* NVIT02

Based on *16S* rRNA gene analysis and whole genome sequencing, we identified NVIT01 as most closely related to *S. marcescens* UMH8, and NVIT02 most closely related to *P. protegens* Cab57/CHA0 (Figure 4A), the latter of which were previously known to possess atrazine degradation genes (Udiković-Kolić et al., 2012) and are observed to be active in our above metatranscriptomic sequencing analysis. In nature, there are a number of soil and water bacteria genera that can metabolize atrazine, including *Pseudomonas*, *Arthrobacter*, *Nocardioides*, *Agrobacterium*, *Comamonas*, *Rhodobacter*, and *Acinetobacter* (Udiković-Kolić et al., 2012). Currently, two atrazine biodegrading pathways have been characterized. The Atz pathway contains *atzA*, *B*, *C*, *D*, *E* and *F* genes encoding enzymes for metabolism of this herbicide (Udiković-Kolić et al., 2012). The other known pathway is Trz, containing *trzN*, *D*, and *F* genes that encode for enzymes capable of metabolizing atrazine (Udiković-Kolić et al., 2012) (Figure 4B). To further assess the functional roles of *S. marcescens* NVIT01 and *P. protegens* NVIT02, we performed whole genome analysis (Table S6) and PCR targeting previously described atrazine metabolism genes.

Aligning the predicted atrazine A homolog gene from *S. marcescens* NVIT01 (*atzA-ser*) with other amidohydrolase superfamily members, we found a conserved pattern consisting of an HXH motif (Figure 4C), where H is histidine, and X is a varying amino acid (Holm and Sander, 1997; Sadowsky et al., 1998). Thus, although the low homology of *atzA-ser* compared with *atzA* (22%) or *trzN* (25%) (Table 1), it retains conserved functional domains. The putative *atzA*, *C, E, F* genes had only a 22% - 51% amino acid identity compared with known Atz/Trz pathways genes (Table 1). These results indicate a potentially different degradation pathway that needs to be studied and verified in future experiments.

P. protegens NVIT02 possessed the predicted genes *atzA*, *B*, *C*, which are 100%, 100%, and 99% similar to *Pseudomonas sp.* ADP, respectively, as assessed by PCR (Table 1). The high gene similarities indicate that the *P. protegens* NVIT02 atrazine degradation pathway may closely resemble the known pathway of *Pseudomonas sp*. ADP, which is plasmid borne and only

contains *atzA*, *B*, and *C* to degrade atrazine to cyanuric acid (de Souza et al., 1998). These genes were also detected from the DNA template of whole *N. vitripennis* and from bacteria grown in atrazine minimal media (Table 1). Using known primers, we did not detect any previously described atrazine-degradation genes in pure *S. marcescens* NVIT01 cultures (Table 1). Homologs to atrazine genes in the *S. marcescens* NVIT01 draft genome were observed, but they were divergent from previously known genes (Table 1). Both bacteria are viable in *Nasonia*, as observed in the *Serratia* and *Pseudomonas* sp. transcripts in our metatranscriptome analysis (Figure S1H).

For *P. protegens* NVIT02, we were unable to detect the *atzD*, *E*, or *F* using known primers. Furthermore, we did not detect any atrazine-degradation genes, including *atzA*, *B*, and *C* from our draft genome (71x coverage). These results provide strong evidence that the *P. protegens* NVIT02 atrazine degradation pathway is encoded through an extrachromosomal element, such as a plasmid, that is present in low copy number. Alternatively, the plasmid may not be critical for survival and is lost in the absence of selective pressures (Bergstrom et al., 2000), as genomic DNA for whole genome sequencing originated from a culture grown in nutrient broth, not atrazine-selective media (see STAR Methods).

Multigenerational Exposure Causes Microbiome-Induced Selection on Host Genome

Because we observed a microbiome shift with a functional and fitness benefit to the host, we investigated how the community was structured across multiple generations. We used targeted amplicon sequencing of the *16S* rRNA gene to assess the compositional changes of microbiome following continued exposure to subtoxic concentration of atrazine. We observed that the microbiome shifted upon early exposure and remained perturbed through successive generations (Figures 5A and 5B, and Table S7). Results from qPCR analysis confirmed that the bacterial abundance was greater in the atrazine-exposed population compared to the control (Figure 5C). Although most taxa are represented in both populations, there is a distinct shift in the abundance of specific taxa across generations, such as the increase in Gammaproteobacteria (Figure 5A). This shift could reflect typical variation of the bacterial communities or the outcome of selection on their hosts' genome and the mechanisms that regulate the microbial community structure.

We used microsatellite analysis to determine if continuous exposure to stressors such as atrazine can cause the populations to significantly diverge across the *Nasonia* genome (Figures 5D and 5E). After five generations, both the control (C_5) and atrazine-exposed (A_5) populations had significantly diverged from the ancestral population (F_1) (Fst = 0.1002 (C_5) $p < 0.05$, and 0.2241 (A_5) $p < 0.01$, Table S8). After thirty generations, the control population (C_{30}) had genetically diverged from the ancestral population (F_1) (Fst = 0.1683, $p < 0.05$, Table S8). The fixation index observed here is very similar to that observed after 36 generations (Fst = 0.26) by van de Zande et al. (2014). However, there is a three-fold change in the genetic differentiation between the atrazine-exposed (A_{30}) and the ancestral population (C_1) (Fst = 0.5403, $p < 0.001$, Table S8) compared to that of the control C_{30} and C_1 (0.1683), indicating a greater selective pressure on the atrazine-exposed population relative to the control.

In this study, we observed near-parallel evolution between the host populations and their associated microbiomes over a short generational timescale, which is consistent with phylosymbiosis—an observation that hosts and their microbiomes reflect divergence between host species (Figure 5F). While there are several reports of phylosymbiosis in literature (Brooks et al., 2016; Moeller et al., 2016), this provides a specific example of experimentally evolved populations undergoing a microbiome-selective pressure. We compared microbial community beta diversity with host microsatellite trees based on Nei's genetic distances (Nei, 1972) across generations of the two experimental populations (control and atrazine diets). The topological similarity was tested using matching cluster (MC) and Robinson-Foulds (RF) metrics (https://eti.pg.edu.pl/treecmp/), where the normalized distances (nMC and nRF) are from 0.0 (complete congruence) to 1.0 (complete incongruence) (Brooks et al., 2016). We observed a significant, although not complete, topological congruency between weighted UniFrac and the host microsatellite tree (nRF 0.2773 with $p = 0.0088$ and nMC 0.3963 with $p = 0.0036$) (Figure 5F). Significant congruence using MC (nMC 0.4755, $p = 0.0183$), and nearly significant congruence using RF (nRF 0.8319, $p = 0.0541$), was detected between Bray-Curtis and host microsatellite trees (Figure 5F). These data are the result of a closed system of experimentally evolved populations with reduced variability and little opportunity to acquire new bacteria. We are unlikely to observe phylosymbiotic congruence for the other two metrics (unweighted UniFrac and Jaccard), as absence and abundance are critical for distinguishing populations (Mazel et al., 2018).

The observation of drift or selection within the population even without atrazine exposure, is potentially due to a founder effect and the addition of sucrose in the control diet of each generation - an uncharacteristic rearing procedure for *Nasonia* generations prior to the described experiments. Given the effective population size of $N_e = 42$, we would expect to observe drift to fixation of allele frequency $p = 0.5$ to occur in 88 generations, or $p = 0.1$ in 40 generations (Kimura and Ohta, 1969). After the fifth generation, the control population diverged modestly, but not significantly, between subsequent generations, while the atrazine-exposed population continued to diverge significantly between subsequent generations (Table S8). This indicates a higher selective pressure on the exposed population and correlates to the shifted microbiome diversity and function.

We did not observe any significant differences in mean gene diversity or allelic richness between the two populations, but there was a clear decrease in both metrics within the atrazine-exposed population (Table S8). This result may reflect the use of a highly inbred standard laboratory strain where the heterozygosity is lower than natural *N. vitripennis* populations (Werren et al., 2010). Taken together, these results suggest the altered microbiome was associated with coevolutionary changes in *N. vitripennis* in the atrazine-exposed and control populations and could be causal in the selection observed at the level of host population genetics.

DISCUSSION

In this study, we observed that environmentally relevant concentrations of atrazine altered the microbiome density and structure

Table 1. Comparison of Atrazine-Metabolizing Genes Relevant to the Current Study

ATZ metabolizing gene	*Serratia marcescens* NVIT01[a]	*Pseudomonas protegens* NVIT02[b]	*Nasonia virtipennis*[c]	*Apis mellifera*[b]	*Eucera hamata*[b]	Atz pathway	Trz pathway
atzA	22%	MG592715	MG592715	MK312633	MK312637	AAK50270 (*Pseudomonas sp.* ADP)	AAL39016 (*Nocardioides sp.* C190)
trzN	25%	100%	100%	99%	99%		
atzB	-	MG592716	MG592716	MK312634	MK312638	AAC45138 (*Pseudomonas sp.* ADP)	
		100%	100%	100%	100%		
atzC	28%	MG592717	MG592717	MK312635	MK312639	AAB96621 (*Pseudomonas sp.* ADP)	
		99%	99%	100%	100%		
atzD	-	-	-	-	-	AAK50331 (*Pseudomonas sp.* ADP)	AAC61577 (*Pseudomonas sp.* NRRLB-12227)
trzD							
atzE	39%	-	-	-	-	AAK50332 (*Pseudomonas sp.* ADP)	
atzF	51%	-	-	-	-	AAK50333 (*Pseudomonas sp.* ADP)	AAK11683 (*Enterobacter cloacae* 99)
trzF	51%						

-Failure to detect the gene from bacteria draft genome and PCR amplification.

[a]The amino acid similarity compared with Atz pathway and Trz pathway. All the genes are from draft genome.

[b]The amino acid similarity compared with Atz pathway. All the genes are from PCR amplification

[c]The amino acid similarity compared with Atz pathway. All the genes are from PCR amplification and are identical with sequences from *Pseudomonas protegens* NVIT02.

in *N. vitripennis* and directly impacted survival. The exposure to atrazine had an impact on the composition of the microbiome directly on the microbiome or alterations of host response and other microbiome regulatory mechanisms (Chu and Mazmanian, 2013). By the eighth generation, we observed a significant increase in tolerance to atrazine in the atrazine-exposed population compared to the control. These lab based observations of microbiome mediated resistance are likely retained microbiome functions that could serve other roles in the microbiome or host physiology, but both bacteria and their associated atrazine metabolic function has been observed in wild caught *Nasonia* (data unpublished, care of Elena Dalla Benettta and Leo Bukeboom of the University of Groningen). The most commonly reported mechanisms leading to insecticide resistance are physical, metabolic, or target site resistance of the host, all of which usually evolve over longer periods of time than those used in this study (Callaghan, 1991). In contrast, symbiont-mediated resistance may occur more quickly; however, there has been only a few cases reported to date (Itoh et al., 2018). In our study, we observed an immediate disruption in microbiome structure and an increase in microbial load following atrazine exposure. The subsequent microbial community shift ultimately supports a symbiont-mediated resistance mechanism in subsequent generations.

Wild populations of pollinators have been exposed to atrazine since the 1950's, the equivalent of dozens of generations, which could have undergone similar microbiome mediated resistance and subsequent host adaptation. For example, we observed that 60% of wild bee samples (*A. mellifera* and *Eucera hamata*) collected from around fields that had been sprayed with atrazine were detected bacterial atrazine-metabolizing genes (Table 1). The atrazine metabolizing genes in bees are mostly likely from the bees' gut bacteria since the *A. mellifera* genome lack homologous atrazine metabolizing genes. These results could reflect events of microbe-host-associated changes in response to xenobiotic exposure in wild honeybee population, similar to what we describe in *Nasonia* and considering the decades of habitual exposure, and adaptation within pollinator populations are likely to have already occurred. As we have demonstrated, the multi-generational impact of even subtoxic exposure could be related to species' tolerances to various xenobiotics or even responsiveness to pathogens. Ultimately, these effects could have repercussions on host behavior, metabolic stress, immunocompetence, and host-microbiota regulation. Likewise, when we analyzed metatranscriptome data from the human fecal microbiome we observed similar atrazine degrading mechanism expressed (Abu-Ali et al., 2018), broadening the implications of exposure to xenobiotics in the human food chain.

The tight association of host selection in response to microbiome shifts, which are themselves a response to environmental factors, indicates that these populations act more congruous as a unit of cooperation (hologenome concept) than a truly Darwinian individual (Stencel and Wloch-Salamon, 2018). Our study is one of the few cases to experimentally evolve cooperation between a host animal and rare members of the microbiome to derive new fitness traits within the population. The hologenome concept of evolution predicts that species can and do evolve in the presence of phenotypic traits derived from microbiome cooperation as reinforced by natural selection (Soen, 2014; Stencel and Wloch-Salamon, 2018). The hologenome

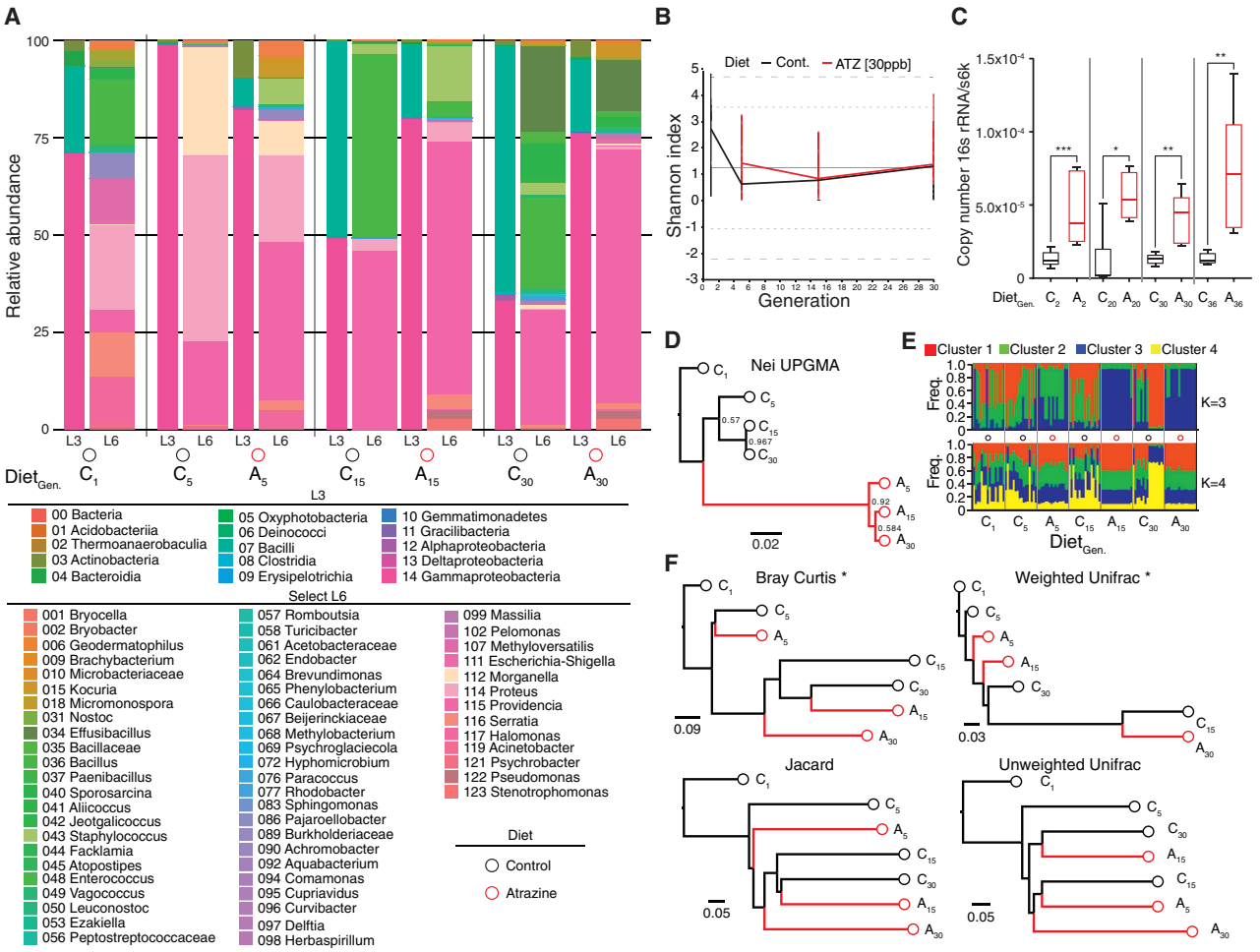

Figure 5. Atrazine Exposure Affects Host Microbiome and Host Genome

(A) The relative abundance of gut bacterial taxa identified at nearest class (L3) and nearest genus levels (L6) (n = 11, 7, 13, 13, 10, 14, 16 for C_1, C_5, A_5, C_{15}, A_{15}, C_{30}, A_{30}, respectively). Replicates are grouped via mean-ceiling.

(B) Volatility chart of longitudinal change in Shannon index between control and atrazine populations.

(C) Total microbiome density in atrazine-exposed and control populations after atrazine and control diets, respectively (the total bacterial *16S* rRNA gene copies relative to *N. vitripennis* single copy gene *S6K* using qPCR). Box-and-whisker plots show max, min, and median values, respectively. *$p < 0.05$, **$p < 0.01$, ***$p < 0.001$; Mann-Whitney U test.

(D) Nei's standard genetic distance phylogenetic tree of different populations of microsatellites.

(E) Genetic structure of different populations based on Bayesian clustering approach. The number of populations (K = 3 and 4) and population ID are shown.

(F) Beta diversity analysis of microbial communities for the generations to compare with the host phylogeny (*$p < 0.05$ for nRF and nMC tests for congruency).

concept is controversial but testable through experimental evolution, in part because it is a variation of existing genome x genome x environment frameworks into a host-microbiome (as genome) x environment—requiring a change in conceptual silos (Stencel and Wloch-Salamon, 2018). However, using our naive and exposed populations as reproductively isolated populations, we can test the validity of the host-microbiome function and structure across generations to determine if the microbiota response to the environmental stressor (atrazine) can fix changes in the host-microbiome relationship, either through host regulatory mechanisms or through gain/loss of function in the microbial community itself. Further studies of the phenotypic changes that might result in reproductive isolation between these experimentally derived populations would drive home the ratchetting effect of the hologenome unit of selection.

Here, we demonstrate a scenario in which changes to the diet of an organism can impact the microbial community, which can in turn directly impact host fitness across generations. However, a number of intriguing questions remain: How does *N. vitripennis* control/transmit the enriched bacteria? How do these two bacteria interact with other symbionts? Are other bacterial taxa involved in host resistance? How will host-microbiome cross-talk co-evolve and become fixed over time? Despite these questions, it is clear that xenobiotic-induced changes to the microbiome have a lasting impact on the fitness of subsequent generations. Further host-microbiome studies of multi-generational exposure to xenobiotic compounds are needed, especially in light of the increased risk of xenobiotic exposure to humans, plants, animals, fungi, and bacteria across the globe.

STAR★METHODS

Detailed methods are provided in the online version of this paper and include the following:

- KEY RESOURCES TABLE
- LEAD CONTACT AND MATERIALS AVAILABILITY
- EXPERIMENTAL MODEL AND SUBJECT DETAILS
  - *Nasonia* Rearing
  - Germ-free Rearing
  - Microbiota Preparation
  - Bacterial Enrichment and Isolation
  - Field Collection of *A. mellifera* and *E. hamata*
- METHOD DETAILS
  - Measurement of Median Lethal Concentration (LC50)
  - Sample Collection and DNA/RNA Extraction
  - PCR, Library Prep, and Sequencing for Microbiome Studies
  - Microbiome Analysis
  - Phylosymbiosis Analysis
  - qPCR Analysis
  - RNA Sequencing and Analysis
  - Proteomic Analysis
  - Database Search and Protein Quantification
  - Microsatellite Analysis
  - Bioluminescence Assay
  - LCMS Assay
  - Identification of Atrazine-Degrading Bacterial Strains and Genes
  - Bacterial Genome DNA Preparation, Sequencing, and Analysis
  - Bacterial Feeding for Probiotic Assay
- QUANTIFICATION AND STATISTICAL ANALYSIS
  - General
  - Quantification of Gene Expression
  - Quantification of Protein Expression
  - Quantification of Phylogeny Congruency
- DATA AND CODE AVAILABILITY

SUPPLEMENTAL INFORMATION

Supplemental Information can be found online at https://doi.org/10.1016/j.chom.2020.01.009.

ACKNOWLEDGMENTS

We thank Jessica Dittmer and Amulya Shastry for their assistance in the early analysis of the microbiome and RNA-seq data sets. We also thank Bojana Jovanovic for facilitating portions of the sequencing experiments as well as revisions of the manuscript. We thank Dr. Emily Balskus (Harvard University), Dr. Reid Harris (James Madison University), Dr. Nate Cira (Rowland Institute at Harvard University), Dr. Colleen Cavanaugh (Harvard University), Dr. Tamar Aprahamian (JetPub Scientific Communications) and Dr. Seth Bordenstein (Vanderbilt University) for reviewing early drafts of the manuscript and in the preparation of this manuscript. We thank Dr. Julia Schwartzman (Gilmore lab, Harvard Medical School) for assistance with the bioluminescence assay. We thank Dr. Bogdan Budnik from the Mass Spectrometry and Proteomics Resource Laboratory (Harvard University) for providing the proteomics raw data report. We thank Dr. James Foley (Rowland Institute, Harvard University) for sharing equipment. We thank Dr. Marie-José Durand (Nantes University, France) for providing *E.coli* SM004 for use in the atrazine bioassay. This work was supported by the Rowland Institute at Harvard Fellowship awarded to RMB.

AUTHOR CONTRIBUTIONS

R.M.B. designed and conducted the experiments, analyzed the data, and wrote the manuscript. G.-H.W. conducted and analyzed experiments and wrote the manuscript. B.M.B. assisted with analysis and wrote the manuscript. O.V. assisted with the experiments and data analysis. N.J. assisted with Kraken 2 analysis of metatranscriptome data, and the dark-field microscopy was conducted by R.M.B. and N.J. with a special thanks for Katja Taute at the Rowland institue for initial imaging support. S.A. and K.P.C.M. conducted the analytical chemistry and manuscript revisions.

DECLARATION OF INTERESTS

The authors declare no competing interests.

Received: September 23, 2019
Revised: November 26, 2019
Accepted: January 15, 2020
Published: February 4, 2020

REFERENCES

Abu-Ali, G.S., Mehta, R.S., Lloyd-Price, J., Mallick, H., Branck, T., Ivey, K.L., Drew, D.A., DuLong, C., Rimm, E., Izard, J., et al. (2018). Metatranscriptome of human faecal microbial communities in a cohort of adult men. Nat. Microbiol. *3*, 356–366.

Al Naggar, Y., Wiseman, S., Sun, J., Cutler, G.C., Aboul-Soud, M., Naiem, E., Mona, M., Seif, A., and Giesy, J.P. (2015). Effects of environmentally-relevant mixtures of four common organophosphorus insecticides on the honey bee (*Apis mellifera* L.). J. Insect Physiol. *82*, 85–91.

Badejo, M.A., and Vanstraalen, N.M. (1992). Effects of atrazine on growth and reproduction of Orchesella-Cincta (Collembola). Pedobiologia (Jena) *36*, 221–230.

Baker, N.T., and Stone, W.W. (2015). Estimated annual agricultural pesticide use for counties of the conterminous United States, 2008–12. US Geological Survey Data *907*, 9.

Bellini, M.I., Pinelli, L., Dos Santos, M.E., and Scavino, A.F. (2014). Bacterial consortia from raw water and sludges from water potabilization plants are able to degrade atrazine. Int. Biodeterior. Biodegradation *90*, 131–139.

Belloni, V., Dessì-Fulgheri, F., Zaccaroni, M., Di Consiglio, E., De Angelis, G., Testai, E., Santochirico, M., Alleva, E., and Santucci, D. (2011). Early exposure to low doses of atrazine affects behavior in juvenile and adult CD1 mice. Toxicology *279*, 19–26.

Bergstrom, C.T., Lipsitch, M., and Levin, B.R. (2000). Natural selection, infectious transfer and the existence conditions for bacterial plasmids. Genetics *155*, 1505–1519.

Blacket, M.J., Robin, C., Good, R.T., Lee, S.F., and Miller, A.D. (2012). Universal primers for fluorescent labelling of PCR fragments–an efficient and cost-effective approach to genotyping by fluorescence. Mol. Ecol. Resour. *12*, 456–463.

Bolyen, E., Rideout, J.R., Dillon, M.R., Bokulich, N.A., Abnet, C.C., Al-Ghalith, G.A., Alexander, H., Alm, E.J., Arumugam, M., Asnicar, F., et al. (2019). Reproducible, interactive, scalable and extensible microbiome data science using QIIME 2. Nat. Biotechnol. *37*, 852–857.

Brodkin, M.A., Madhoun, H., Rameswaran, M., and Vatnick, I. (2007). Atrazine is an immune disruptor in adult northern leopard frogs (*Rana pipiens*). Environ. Toxicol. Chem. *26*, 80–84.

Brooks, A.W., Kohl, K.D., Brucker, R.M., van Opstal, E.J., and Bordenstein, S.R. (2016). Phylosymbiosis: relationships and functional effects of microbial communities across host evolutionary history. PLoS Biol. *14*, e2000225.

Brucker, R.M., and Bordenstein, S.R. (2013). The hologenomic basis of speciation: gut bacteria cause hybrid lethality in the genus *Nasonia*. Science *341*, 667–669.

Callaghan, A. (1991). Insecticide resistance - mechanisms and detection methods. Sci. Prog. *75*, 423–437.

Chu, H., and Mazmanian, S.K. (2013). Innate immune recognition of the microbiota promotes host-microbial symbiosis. Nat. Immunol. *14*, 668–675.

Cole, J.R., Wang, Q., Fish, J.A., Chai, B., McGarrell, D.M., Sun, Y., Brown, C.T., Porras-Alfaro, A., Kuske, C.R., and Tiedje, J.M. (2014). Ribosomal Database Project: data and tools for high throughput rRNA analysis. Nucleic Acids Res. *42*, D633–D642.

de Souza, M.L., Wackett, L.P., and Sadowsky, M.J. (1998). The *atzABC* genes encoding atrazine catabolism are located on a self-transmissible plasmid in *Pseudomonas* sp. strain ADP. Appl. Environ. Microbiol. *64*, 2323–2326.

Dierickx, P.J. (1999). Glutathione-dependent cytotoxicity of the chloroacetanilide herbicides alachlor, metolachlor, and propachlor in rat and human hepatoma-derived cultured cells. Cell Biol. Toxicol. *15*, 325–332.

Dobin, A., and Gingeras, T.R. (2015). Mapping RNA-seq reads with STAR. Curr. Protoc. Bioinformatics *51*, https://doi.org/10.1002/0471250953.bi1114s51.

Douglas, A.E. (2015). Multiorganismal insects: diversity and function of resident microorganisms. Annu. Rev. Entomol. *60*, 17–34.

Folmer, O., Black, M., Hoeh, W., Lutz, R., and Vrijenhoek, R. (1994). DNA primers for amplification of mitochondrial cytochrome c oxidase subunit I from diverse metazoan invertebrates. Mol. Mar. Biol. Biotechnol. *3*, 294–299.

Guindon, S., Dufayard, J.F., Lefort, V., Anisimova, M., Hordijk, W., and Gascuel, O. (2010). New algorithms and methods to estimate maximum-likelihood phylogenies: assessing the performance of PhyML 3.0. Syst. Biol. *59*, 307–321.

Holm, L., and Sander, C. (1997). An evolutionary treasure: unification of a broad set of amidohydrolases related to urease. Proteins *28*, 72–82.

Horzmann, K.A., Reidenbach, L.S., Thanki, D.H., Winchester, A.E., Qualizza, B.A., Ryan, G.A., Egan, K.E., Hedrick, V.E., Sobreira, T.J.P., Peterson, S.M., et al. (2018). Embryonic atrazine exposure elicits proteomic, behavioral, and brain abnormalities with developmental time specific gene expression signatures. J. Proteomics *186*, 71–82.

Hua, A., Gueuné, H., Cregut, M., Thouand, G., and Durand, M.J. (2015). Development of a bacterial bioassay for atrazine and cyanuric acid detection. Front. Microbiol. *6*, 211.

Huang, W., Sherman, B.T., and Lempicki, R.A. (2009). Systematic and integrative analysis of large gene lists using DAVID bioinformatics resources. Nat. Protoc. *4*, 44–57.

Itoh, H., Tago, K., Hayatsu, M., and Kikuchi, Y. (2018). Detoxifying symbiosis: microbe-mediated detoxification of phytotoxins and pesticides in insects. Nat. Prod. Rep. *35*, 434–454.

Käll, L., Storey, J.D., and Noble, W.S. (2008). Non-parametric estimation of posterior error probabilities associated with peptides identified by tandem mass spectrometry. Bioinformatics *24*, i42–i48.

Kikuchi, Y., Hayatsu, M., Hosokawa, T., Nagayama, A., Tago, K., and Fukatsu, T. (2012). Symbiont-mediated insecticide resistance. Proc. Natl. Acad. Sci. USA *109*, 8618–8622.

Kimura, M., and Ohta, T. (1969). The Average Number of Generations until Fixation of a Mutant Gene in a Finite Population. Genetics *61*, 763–771.

Knutie, S.A., Gabor, C.R., Kohl, K.D., and Rohr, J.R. (2018). Do host-associated gut microbiota mediate the effect of an herbicide on disease risk in frogs? J. Anim. Ecol. *87*, 489–499.

Koevoets, T., Niehuis, O., van de Zande, L., and Beukeboom, L.W. (2012). Hybrid incompatibilities in the parasitic wasp genus *Nasonia*: negative effects of hemizygosity and the identification of transmission ratio distortion loci. Heredity *108*, 302–311.

Le Goff, G., Hilliou, F., Siegfried, B.D., Boundy, S., Wajnberg, E., Sofer, L., Audant, P., ffrench-Constant, R.H., and Feyereisen, R. (2006). Xenobiotic response in *Drosophila melanogaster*: sex dependence of P450 and GST gene induction. Insect Biochem. Mol. Biol. *36*, 674–682.

Lim, S., Ahn, S.Y., Song, I.C., Chung, M.H., Jang, H.C., Park, K.S., Lee, K.U., Pak, Y.K., and Lee, H.K. (2009). Chronic exposure to the herbicide, atrazine, causes mitochondrial dysfunction and insulin resistance. PLoS One *4*, e5186.

Love, M.I., Huber, W., and Anders, S. (2014). Moderated estimation of fold change and dispersion for RNA-seq data with DESeq2. Genome Biol. *15*, 550.

Mannix, M. (2016). Atrazine Registration Review, E.P. Agency, ed. (EPA-HQ-OPP), 2013–0266.

Mazel, F., Davis, K.M., Loudon, A., Kwong, W.K., Groussin, M., and Parfrey, L.W. (2018). Is Host Filtering the Main Driver of Phylosymbiosis across the Tree of Life? mSystems *3*, e00097-18.

McCallum, M.L., Matlock, M., Treas, J., Safi, B., Sanson, W., and McCallum, J.L. (2013). Endocrine disruption of sexual selection by an estrogenic herbicide in the mealworm beetle (Tenebrio molitor). Ecotoxicology *22*, 1461–1466.

Moeller, A.H., Caro-Quintero, A., Mjungu, D., Georgiev, A.V., Lonsdorf, E.V., Muller, M.N., Pusey, A.E., Peeters, M., Hahn, B.H., and Ochman, H. (2016). Cospeciation of gut microbiota with hominids. Science *353*, 380–382.

Motta, E.V.S., Raymann, K., and Moran, N.A. (2018). Glyphosate perturbs the gut microbiota of honey bees. Proc. Natl. Acad. Sci. USA *115*, 10305–10310.

Nei, M. (1972). Genetic distance between populations. Am. Nat. *106*, 283–292.

Niehuis, O., Büllesbach, J., Judson, A.K., Schmitt, T., and Gadau, J. (2011). Genetics of cuticular hydrocarbon differences between males of the parasitoid wasps *Nasonia giraulti* and *Nasonia vitripennis*. Heredity *107*, 61–70.

Pritchard, J.K., Stephens, M., and Donnelly, P. (2000). Inference of population structure using multilocus genotype data. Genetics *155*, 945–959.

Quast, C., Pruesse, E., Yilmaz, P., Gerken, J., Schweer, T., Yarza, P., Peplies, J., and Glöckner, F.O. (2013). The SILVA ribosomal RNA gene database project: improved data processing and web-based tools. Nucleic Acids Res. *41*, D590–D596.

Robertson, J.L., Russell, R.M., Preisler, H.K., and Savin, N.E. (2007). Bioassays with Arthropods, Second Edition (CRC press).

Rohr, J.R., Sager, T., Sesterhenn, T.M., and Palmer, B.D. (2006). Exposure, postexposure, and density-mediated effects of atrazine on amphibians: breaking down net effects into their parts. Environ. Health Perspect. *114*, 46–50.

Rooney, A.A., Matulka, R.A., and Luebke, R.W. (2003). Developmental atrazine exposure suppresses immune function in male, but not female Sprague-Dawley rats. Toxicol. Sci. *76*, 366–375.

Sadowsky, M.J., Tong, Z., de Souza, M., and Wackett, L.P. (1998). AtzC is a new member of the amidohydrolase protein superfamily and is homologous to other atrazine-metabolizing enzymes. J. Bacteriol. *180*, 152–158.

Soen, Y. (2014). Environmental disruption of host-microbe co-adaptation as a potential driving force in evolution. Front. Genet. *5*, 168.

Stencel, A., and Wloch-Salamon, D.M. (2018). Some theoretical insights into the hologenome theory of evolution and the role of microbes in speciation. Theory Biosci. *137*, 197–206.

Takezaki, N., Nei, M., and Tamura, K. (2010). POPTREE2: Software for constructing population trees from allele frequency data and computing other population statistics with Windows interface. Mol. Biol. Evol. *27*, 747–752.

Thornton, B.J., Elthon, T.E., Cerny, R.L., and Siegfried, B.D. (2010). Proteomic analysis of atrazine exposure in *Drosophila melanogaster* (Diptera: Drosophilidae). Chemosphere *81*, 235–241.

Troll, J.V., Hamilton, M.K., Abel, M.L., Ganz, J., Bates, J.M., Stephens, W.Z., Melancon, E., van der Vaart, M., Meijer, A.H., Distel, M., et al. (2018). Microbiota promote secretory cell determination in the intestinal epithelium by modulating host Notch signaling. Development *145*, https://doi.org/10.1242/dev.155317.

Udiković-Kolić, N., Scott, C., and Martin-Laurent, F. (2012). Evolution of atrazine-degrading capabilities in the environment. Appl. Microbiol. Biotechnol. *96*, 1175–1189.

van de Zande, L., Ferber, S., de Haan, A., Beukeboom, L.W., van Heerwaarden, J., and Pannebakker, B.A. (2014). Development of a *Nasonia vitripennis* outbred laboratory population for genetic analysis. Mol. Ecol. Resour. *14*, 578–587.

Vogel, A., Jocque, H., Sirot, L.K., and Fiumera, A.C. (2015). Effects of atrazine exposure on male reproductive performance in *Drosophila melanogaster*. J. Insect Physiol. *72*, 14–21.

Wang, G.-H., and Brucker, R.M. (2019). Genome Sequence of *Providencia rettgeri* NVIT03, Isolated from *Nasonia vitripennis*. Microbiol Resour Announc *8*, e01157-18.

Watanabe, M., Kojima, H., and Fukui, M. (2014). Proposal of Effusibacillus lacus gen. nov., sp. nov., and reclassification of Alicyclobacillus pohliae as Effusibacillus pohliae comb. nov. and Alicyclobacillus consociatus as Effusibacillus consociatus comb. nov. Int. J. Syst. Evol. Microbiol. *64*, 2770–2774.

Werren, J.H., Richards, S., Desjardins, C.A., Niehuis, O., Gadau, J., Colbourne, J.K., Werren, J.H., Richards, S., Desjardins, C.A., Niehuis, O., et al.; Nasonia Genome Working Group (2010). Functional and evolutionary insights from the genomes of three parasitoid *Nasonia* species. Science *327*, 343–348.

Wood, D.E., and Salzberg, S.L. (2014). Kraken: ultrafast metagenomic sequence classification using exact alignments. Genome Biol. *15*, R46.

Wright, S. (1933). Inbreeding and Homozygosis. Proc. Natl. Acad. Sci. USA *19*, 411–420.

STAR★METHODS

KEY RESOURCES TABLE

REAGENT or RESOURCE	SOURCE	IDENTIFIER
Bacterial and Virus Strains		
E.coli SM004	(Hua et al., 2015)	N/A
Serratia marcescens NVIT01	This study	N/A
Pseudomonas protegens NVIT02	This study	N/A
Biological Samples		
Nasonia vitripennis	(Werren et al., 2010)	AsymCX(u)
Apis mellifera	This study	N/A
Eucera hamata	This study	N/A
Sarcophaga bullata pupae	Seth R. Bordenstein lab	N/A
S. bullata pupae	Carolina Biological Supply	Cat# 173486
Chemicals, Peptides, and Recombinant Proteins		
Atrazine analytical standard	TCI America	Cat# 1912-24-9, $\geq$ 97% purity
Cyanuric acid analytical standard	Sigma-Aldrich	Cat# 108-80-5, for synthesis
Terrific Broth (TB)	HARDY DIAGNOSTICS	Cat# C8151
Lysogeny Broth, Miller (LB)	BD Difco	Cat# 244620
Nutrition Broth (NB)	Millipore Sigma	Cat# 1.05443.0500
Ampicillin	Sigma-Aldrich	Cat# 69-52-3
Gentamicin	Sigma-Aldrich	Cat# 1405-41-0
Glyphosate	Toronto Research Chemicals	Cat# 1071-83-6
Imidacloprid	Toronto Research Chemicals	Cat# 120868-66-8
KH_2PO_4	G-Biosciences	Cat# RC-083
$Na_2HPO_4 \cdot 12H2O$	Sigma-Aldrich	Cat# 71649-500G
$MgSO_4 \cdot 7\ H_2O$	Sigma-Aldrich	Cat# 63138-250G
sodium citrate	Sigma-Aldrich	Cat# 71497-250G
Sucrose	Sigma-Aldrich	Cat# S7903-250G
Isopropyl-b-D-thiogalactopyranoside (IPTG) R 99%	Thermo Fisher Scientific	Cat# BP1755
DNA OUT	G-Biosciences	Cat# 82021-438
UltraPure DNase/RNase Free Distilled Water	Thermo Fisher Scientific	Cat# 10-977-023
Critical Commercial Assays		
Qubit RNA HS Assay Kit	Thermo Fisher Scientific	Cat# Q32852
Qubit dsDNA HS Assay Kit	Thermo Fisher Scientific	Cat# Q32854
DNeasy Blood & Tissue Kit (250)	QIAGEN	Cat# 69506
RNeasy Plus Mini Kit (250)	QIAGEN	Cat# 74136
Plasmid Mini Kit	QIAGEN	Cat#
Q5 High-Fidelity 2X Master Mix - 500 rxns	New England Biolabs (NEB)	Cat# M0492L
TaKaRa Ex Taq DNA Polymerase	Takara Bio	Cat# RR001B
GoTaq Green Master Mix	Promega	Cat# M7123
GoTaq Real-Time qPCR and RT-qPCR Systems for Dye-Based Detection	VWR International	Cat# A6002
Nucleic Acid Purification Systems, Promega, Wizard SV Gel and PCR	VWR International	Cat# PAA9282
Deposited Data		
S. marcescens NVIT01 genome	This study	PEGE00000000 at DDBJ/ENA/GenBank
P. protegens NVIT02 genome	This study	PISQ00000000 at DDBJ/ENA/GenBank
N. vitripennis proteomics	This study	PXD011964 at ProteomeXchange Consortium

(*Continued on next page*)

Continued

REAGENT or RESOURCE	SOURCE	IDENTIFIER
RNA-seq data	This study	PRJNA509675 at NCBI
16S rRNA data	This study	PRJNA509675 at NCBI
LC50 measurement	This study	https://doi.org/10.17632/v3csd6wmh7.1
Microsatellite data	This study	https://doi.org/10.17632/v3csd6wmh7.1
CFU count	This study	https://doi.org/10.17632/v3csd6wmh7.1
HPLC data	This study	https://doi.org/10.17632/v3csd6wmh7.1
Bioluminescence data	This study	https://doi.org/10.17632/v3csd6wmh7.1
Oligonucleotides		
For information regarding normal PCR and QPCR primers	This study	Table S1
16 s library primers	This study	Table S1
CAGGACCAGGCTACCGTG	(Blacket et al., 2012)	Table S1
Microsatellite primers	This study	Table S1
Software and Algorithms		
DESeq2	(Love et al., 2014)	https://bioconductor.org/packages/release/bioc/html/DESeq2.html
R (v3.6.0)	R Core Team	https://www.r-project.org
Python (v2.7.13)	Python Core Team	https://www.python.org
GraphPad Prism 6	GraphPad Software	https://www.graphpad.com/scientific-software/prism/
Python (v3.6.8)	Python Core Team	https://www.python.org
Polo Plus-PC (v2.0)	(Robertson et al., 2007)	https://leora-software.com/
QIIME 2 v.2018.6	(Bolyen et al., 2019)	https://qiime2.org/
FigTree v1.4.2	Andrew Rambaut team	http://tree.bio.ed.ac.uk/software/figtree/
TreeCmp v2.0	Gdansk University of Technology	https://eti.pg.edu.pl/treecmp/
FastQC v0.11.7	Babraham Institute	https://www.bioinformatics.babraham.ac.uk/projects/fastqc/
STAR v2.6.0a	(Dobin and Gingeras, 2015)	https://github.com/STAR-Fusion/STAR-Fusion/wiki/STAR-Fusion-release-and-CTAT-Genome-Lib-Compatibility-Matrix
Proteome Discoverer v2.1.0.81	Thermo Scientific	https://www.thermofisher.com/order/catalog/product/OPTON-30795
GENEMAPPER v4.0	Applied Biosystems	From NGH CCIB DNA Core Facility
FSTAT v2.9.3		https://www2.unil.ch/izea/softwares/fstat.html
POPTREE2	(Takezaki et al., 2010)	http://www.med.kagawa-u.ac.jp/~genomelb/takezaki/poptree2/index.html
STRUCTURE v2.3.4	(Pritchard et al., 2000)	https://web.stanford.edu/group/pritchardlab/structure_software/release_versions/v2.3.4/html/structure.html
PhyML v3.0	(Guindon et al., 2010)	http://phylogeny.lirmm.fr/phylo_cgi/one_task.cgi?task_type=phyml
Graph Pad Prism v7.01	GraphPad Software	https://www.graphpad.com/scientific-software/prism/
Other		
DAVID v6.7	(Huang et al., 2009)	https://david.ncifcrf.gov/
SILVA's *16S* QIIME database v132	(Quast et al., 2013)	http://www.metagenomics.wiki/tools/16s/qiime/otu-clustering/silva

LEAD CONTACT AND MATERIALS AVAILABILITY

Further information and requests for resources and reagents should be directed to and will be fulfilled by the Lead Contact, Robert M. Brucker (brucker@rowland.harvard.edu). This study did not generate new unique reagents.

EXPERIMENTAL MODEL AND SUBJECT DETAILS

Nasonia Rearing

The *N. vitripennis* strain AsymCX(u) (*Wolbachia* free) (Werren et al., 2010) was used to establish experimental populations. The atrazine (ATZ) population was fed 30 ppb atrazine in a 10% (w/v) sucrose solution while the control population was fed a control diet of 10% sucrose. Wasps were fed for 48 h, then the food was removed and the adults were provided with 25 *Sarcophaga bullata* pupae (fly hosts) for 48 h. Within each lineage, all pupae were collected, mixed, and randomly sorted into groups of 50 females and 15 males for the next generation. The effective population size (N_e) is 42 based on $N_e = 9\ N_m N_f/(4N_m + 2N_f)$ (Wright, 1933). All *N. vitripennis* were reared in 25°C incubators with constant light. The *S. bullata* fly pupae were from the Seth R. Bordenstein lab (Vanderbilt University, USA) and Carolina Biological Supply (Burlington, NC). All fly hosts color and firmness were checked before providing them to adult *N. vitripennis.* The generation time for *N. vitripennis* under these rearing conditions is approximately two weeks. After 25 generations (F_{25}) each linage was split into additional sub lineages and the diet was switched for subsequent generations.

Germ-free Rearing

All GF rearing was conducted following the protocol set forth by Brucker and Bordenstein (2013) with slight modifications; host *S. bullata* fly pupae were first strained through a 100 μm mesh before centrifugation and no cell culture media or antibiotics were used, volume differences were made up using sterile water. GF media was stored at 4°C for 2 weeks maximum.

Microbiota Preparation

Microbiota were purified from L4 larvae by homogenization of larvae in sterile 1 X PBS. The larval homogenate was then centrifuged at 1000 rpm for 3 min to remove large cellular debris, and the resulting supernatant was filtered through a 5 um filter. The filtrate was centrifuged at 6,000 rpm for 5 min, and the supernatant was removed. The pellet was resuspended in sterile PBS. The microbiomes were then inoculated onto GF L4 larvae during a media feeding. The surviving adults were then fed atrazine or a control diet as described in the LC_{50} procedure.

Bacterial Enrichment and Isolation

Five *N. vitripennis* individuals were homogenized in a single tube with 5 mL AMSM (50 ppm atrazine) and the resulting inoculum was incubated for five days at 250 rev/min at 30°C. Then, 1 mL of enrichment culture was inoculated into fresh AMSM (5 ml) where the atrazine concentration was increased by 50 ppm. This process was repeated six times and the atrazine concentration was increased by 50 ppm each time, to a final concentration of 300 ppm. The final culture was plated on LB agar. Mixed cultures were repeatedly sub-cultured on to new AMSM plates and isolated to obtain pure cultures. A variety of different colonies were selected based on morphology and transferred to LB plates containing atrazine (300 ppm). The plates were incubated for several days at 30°C and periodically examined for zone of clearing. The isolates were also sub-cultured in liquid MSM and AMSM (30 ppb atrazine) for 24 h and then plated on LB. Isolates that grew to a higher density in the presence of atrazine and demonstrated zones of clearing were chosen for further evaluation.

Field Collection of *A. mellifera* and *E. hamata*

In the Spring of 2016, field collections of *A. mellifera* (honeybees) and *E. hamata* were collected in cornfields of Morrow county and Gallia county in central and southern Ohio, USA. Samples were collected one week to two days before the application of atrazine, and 12-14 days after its application. Specimens of *A. mellifera* and *E. hamata* were morphologically identified and confirmed by sequencing a partial fragment of cytochrome *c* oxidase subunit I (*COI*) with the primers LCO1490 and HCO2198 (Folmer et al., 1994) as shown in Table S1. Samples were preserved in 100% molecular grade ethanol when shipped on ice. DNA was extracted, amplified, and sequenced as described above.

METHOD DETAILS

Measurement of Median Lethal Concentration (LC50)

Twenty to fifty yellow/black pupae were kept in a vial and for 24 h, then unemerged and dead pupae were removed and adults were fed varying concentrations of atrazine or glyphosate (0, 3 ppm, 10 ppm, 30 ppm, 100 ppm, 200 ppm, 300 ppm, 600 ppm, 800 ppm, 900 ppm), or 0, 24 ppb, 120 ppb, 600 ppb, 3 ppm of imidacloprid. During GF experiments, *N. vitripennis* adults were fed atrazine at concentrations of 0 and 30 ppm (Figure 1A) and 3 ppm (Figure 2D). All conditions had at least two replicates per condition. Mortality was recorded after 0, 24, 48, 72, 96, 120, 144, and 168 h following atrazine exposure, and after 96 h following glyphosate and imidacloprid exposure. A concentration-response curve was generated and the best fit determined by Probit Analysis using Polo Plus-PC (Robertson et al., 2007). Resistance ratios were calculated by dividing the LC_{50} of the atrazine population by the LC_{50} of the same generation's control population using Polo Plus-PC software, Version: 2.0. Confidence intervals for resistance ratios were calculated by the method described in Robertson et al. (2007). Resistance ratios were compared across conditions to test the significance of resistance ratios at a 95% level CI. A difference between compared values is considered significant if the 95% CI does not include 1.0 (Robertson et al., 2007).

Sample Collection and DNA/RNA Extraction

The founders for each generation of *N. vitripennis* were collected in one tube and subsequently maintained at −80°C until DNA and RNA extraction. For DNA extraction, each individual was put in 1.5 mL tube and rinsed once with 1ml 70% ETOH, then 1ml 10% bleach, and twice with 1ml sterile water. Samples were then frozen in liquid nitrogen with additional mechanical homogenization. All samples were processed for DNA extraction using the DNeasy Blood & Tissue Kit (QIAGEN, Hilden, Germany) according to the manufacturer's instructions. Samples were quantified using the dsDNA HS Assay kit on the Qubit 2.0 Fluorometer (Life Technologies). For RNA extraction, five individual wasps were pooled and crushed to fine powder under liquid nitrogen. Total RNA was extracted using AllPrep DNA/RNA Mini Kit (QIAGEN, Hilden, Germany) according to manufacturer's protocol. We further purified our samples using DNase I (RNase-free, HC, Life Technologies, Waltham, USA). We quantified RNA using RNA HS Assay Kit (Life Technologies, Waltham, USA) on the Qubit 2.0 Fluorometer (Life Technologies, Waltham, USA) and qualified using a NanoDrop 2000/2000c Spectrophotometer (Life Technologies, Waltham, USA).

PCR, Library Prep, and Sequencing for Microbiome Studies

A portion of the *16S* rRNA gene was PCR amplified from 4 μL DNA using the 27F and V4R (5′- GGACTACHVGGGTWTCTAAT-3′) primers. Duplicate reactions per sample were performed using NEB Next High-Fidelity 2X PCR Master Mix in a total reaction volume of 20 μl, 50°C annealing temperature, and 25 cycles. The resulting PCR products were used for a nested-PCR reaction using modified paired primers (Brooks et al., 2016) (Table S1). PCR was performed using two microliters of the previous PCR product in a 20 μL reaction using the NEB Next High-Fidelity 2X PCR Master Mix, with only 12 cycles. Products were purified using Agencourt AMPure XP, quantified using the NanoDrop 2000/2000c Spectrophotometers (Life Technologies, Waltham, USA) and then samples were pooled together. Each pooled library was run on the Illumina MiSeq using the MiSeq Reagent Kit V3 for paired-end reads. Sequencing was performed by the Dana-Farber Cancer Institute, Harvard Medical School.

Microbiome Analysis

Raw Illumina sequence reads were processed using QIIME 2 v.2018.6 (Bolyen et al., 2019). Sequences were joined using the VSEARCH plugin (Bolyen et al., 2019) and filtered using Deblur (Bolyen et al., 2019). Open-reference picking for OTUs was performed using VSEARCH and clustered at 99% identity using SILVA's *16S* QIIME database (v.132) (Quast et al., 2013). Low abundance OTUs (frequency < 10) were filtered and removed across all sampleSQIIME2's Naive Bayes classifier was trained using the SILVA *16S* rRNA Database (v.132, 99% consensus taxonomy, 7 levels) using the q2-feature-classifier (Bolyen et al., 2019). The full-length *16S* trained classifier was used to generate taxonomic classification using the classify-sklearn feature-classifier plugin (Bolyen et al., 2019). ANCOM analysis was conducted to identify taxa of significance between populations.

The taxa plugin was used to remove all unassigned, chloroplasts, mitochondria, and *Wolbachia* from the dataset (taxa filter-table command). Any library sequence lower than 1000 was removed and left libraries were normalized by rarefying the sequencing depth to 1028 (Figures 1 and S4), 1020 (Figures 5 and S4) to correct uneven sequencing depth. Representative sequences were used for alignments with MAFFT (Alignment MAFFT plugin) (Bolyen et al., 2019), with unconserved and highly gapped regions masked (alignment plugin, mask command). Maximum likelihood phylogenetic trees were generated with FastTree 2 (Phylogeny plugin) and midpoint rooted (Phylogeny plugin, midpoint-root option). Following the generation of OTUs, taxonomy assignment, gene alignment, and diversity metrics were generated for each sample using QIIME 2's diversity plug-in (core-metrics command, phylogenetic option). Simpson's index was calculated separately using the diversity plugin (command alpha with Simpson metric). Sample replicates were grouped based on generation (generation 5 = generations 5 and 8, generation 15 = generations 15 and 20, generation 30 = generations 30 and 32) using the feature-table group command (mean-ceiling option). The new grouped feature-table was used for alpha and beta-diversity tests and to generate tree files (Bray-Curtis, Jaccard, Unweighted Unifrac, and Weighted Unifrac) using the diversity plugin (beta-rarefaction command). Volatility was calculated using longitudinal plugin.

Phylosymbiosis Analysis

Following Brooks et al. (2016) to calculate statistics, we re-rooted host and microbiota phylogeny trees using FigTree v1.4.2 (http://tree.bio.ed.ac.uk/software/figtree/). We used TreeCmp 2.0 (https://eti.pg.edu.pl/treecmp/) to quantify the congruency analyses between host phylogeny and microbiota topology. The normalized Robinson-Foulds score and normalized matching cluster score were calculated to determine similarity of the two topologies from 0 (complete congruence) to 1 (incomplete incongruence) (https://eti.pg.edu.pl/treecmp/).

qPCR Analysis

qPCR was performed using a StepOnePlus Real-Time PCR System (Thermo Fisher Scientific, Waltham, U.S.A.). All the primers are listed in Table S1. Reactions consisted of 3 μL of template, 10 μL of GoTaq qPCR Master Mix (Promega, Madison, USA), one microliter of primer mix (10 mM), and 6 μL of sterile water for a total volume of 20 μl. A no-template control was included in each run to check for reagent contamination. A melting curve analysis was performed for each run to confirm the amplification specificity. The thermal conditions were: 40 cycles of 95°C for 10 s, 55 or 60°C for 30 s, and 72°C for 20 s. Two technical replicates were performed for each qPCR assay.

To quantify the presence of target genes, we prepared standard solutions. The PCR amplicons of each gene of interest were purified using Agencourt AMPure XP, and then cloned into Invitrogen pCR2.1-TOPO vector with TOPO10 One Shot Chemically

Competent cells. The plasmids were then prepared with QIAGEN Plasmid Mini Kit (QIAGEN, Hilden, Germany), and quantified with a dsDNA HS Assay kit on the Qubit. Standard 10-fold dilution series from 10^7 to 10^3 copies were prepared and used to calculate the gene copy number.

RNA Sequencing and Analysis

All samples were run multiplexed on the Illumina HiSeq2500 (single-end, 50 bp reads) at Genewiz, Inc. (South Plainfield, NJ). Raw reads were trimmed using FastQC 0.11.7 (Babraham Institute) and mapped using STAR 2.6.0a (Dobin and Gingeras, 2015) to the *N. vitripennis* genome Nvit_2.1 (GCF_000002325.3). Table S3 is a summary of reads per sample and the percentage of mapped reads. Significant differential gene expression was determined using DESeq2 (Love et al., 2014). The gene raw read count and statistics of expression are in Table S3. A gene with a fold change > 1.5 (upregulated) or < 0.67 (downregulated) and P value < 0.05, FDR < 0.05 was considered to be a differentially expressed gene (DEG). Gene ontology (GO) enrichment analysis and Kyoto Encyclopedia of Genes and Genomes (KEGG) pathway enrichment analysis were conducted using the functional annotation tool DAVID 6.7 (Huang et al., 2009). All remaining unassigned reads were retained and analyzed using Kraken 2 (Wood and Salzberg, 2014), version 2.0.7-beta. Briefly, reads were assigned taxonomy by k-mer resemblance to bacterial k-mer profiles using the NCBI genome and chromosome collections (dataset accessed July 16, 2018). Significant taxa abundance was determined from the RNA-seq as described above, based upon relative read abundance for taxa represented at 10 or more reads after unclassified bacterial and *Wolbachia* sequences were removed.

Proteomic Analysis

Individual wasps were immersed in 100 μl total protein proprietary lysis buffer from Covaris in a microTUBE-15 AFA Beads screw-cap (Covaris) and mashed with a yellow pipette tip for six minuteSThe total volume was transferred to a 1.5 mL Eppendorf tube and precipitated using ice-cold methanol/chloroform precipitation. Following precipitation, samples were air-dried and weighed to obtain a relative amount of protein for normalization. Each sample was re-suspended in 200 μl of 50% formic acid, vortexed and centrifuged. Dependent on weighed amount, 200 μg was transferred to a 10 kD centrifugal vial for FASP (Filter Aided Sample Prep) digest. Samples were then labeled with TMT10plex (Thermo-Fisher) and pooled into a single HPLC vial. 10/100 μl was run on LUMOS Mass Spec instrument. Each TMT10plex set was run on the instrument with an identical channel containing an identical pooled sample (control and atrazine-exposed mixture) for normalization.

Each sample was submitted for LC-MS/MS analysis performed on a LTQ Orbitrap Elite (Thermo Fisher) equipped with Waters (Milford, MA) NanoAcquity HPLC pump. Peptides were separated onto a 100 μm inner diameter microcapillary trapping column packed with approximately 5 cm of C18 Reprosil resin (5 μm, 100 Å, Dr. Maisch GmbH, Germany) followed by an analytical column with ~20 cm of Reprosil resin (1.8 μm, 200 Å, Dr. Maisch GmbH, Germany). Separation was achieved by applying a gradient from 5%–27% acetonitrile in 0.1% formic acid over 90 min at 200 nL min^{-1}. Electrospray ionization was enabled through applying a voltage of 1.8 kV using a home-made electrode junction at the end of the microcapillary column and sprayed from fused silica pico tips (New Objective, MA). The LTQ Orbitrap Elite was operated in data-dependent mode for the mass spectrometry methods. The mass spectrometry survey scan was performed in the Orbitrap in the range of 395-1,800 m/z at a resolution of 6×10^4, followed by the selection of the twenty most intense ions (TOP20) for CID-MS2 fragmentation in the Ion trap using a precursor isolation width window of two m/z, AGC setting of 10,000, and a maximum ion accumulation of 200 ms. Singly charged ion species were not subjected to CID fragmentation. Normalized collision energy was set to 35 V with an activation time of 10 ms. Ions in a 10 ppm m/z window around ions selected for MS2 were excluded from further selection for fragmentation for 60 s. The same TOP20 ions were subjected to HCD MS2 event in Orbitrap part of the instrument. The fragment ion isolation width was set to 0.7 m/z, AGC was set to 50,000, the maximum ion time was 200 ms, normalized collision energy was set to 27V with an activation time of one ms for each HCD MS2 scan.

Database Search and Protein Quantification

Raw data were analyzed using Proteome Discoverer 2.1.0.81 (Thermo Scientific) software. Assignment of MS/MS spectra were performed using the Sequest HT algorithm by searching the data against an in-house *N. vitripennis* database, and our *E. coli* K12 database, as well as other known contaminants such as human keratins and common lab contaminants. Sequest HT searches were performed using a 20 ppm precursor ion tolerance and requiring each peptides N-/C termini to adhere with Trypsin protease specificity, while allowing up to two missed cleavageS10-plex TMT tags on peptide N termini and lysine residues (+229.162932 Da) was set as static modifications while methionine oxidation (+15.99492 Da) was set as variable modification. A MS2 spectra assignment protein false discovery rate (FDR) of 1% was achieved by applying the target-decoy database search. Filtering was performed using a Percolator (Käll et al., 2008). For quantification, a 0.02 m/z window centered on the theoretical m/z value of each of the 10 reporter ions and the intensity of the signal closest to the theoretical m/z value was recorded. Each set was run with the same reference sample as an internal standard. The ratios of the relative expression levels between atrazine-exposed and unexposed samples were calculated to compare the relative protein abundances across different samples. A protein with a fold change > 1.2 (upregulated) or < 0.83 (downregulated) and P value < 0.05 (Student's t test) was considered to be differentially regulated.

Microsatellite Analysis

To determine the genetic diversity of the population over time, we isolated DNA from 16 females from the F_1, F_5, F_{15}, and F_{30} from both the atrazine-exposed and control population. DNA was extracted as described above using the DNeasy Blood & Tissue

Kit (QIAGEN, Hilden, Germany). Initial screening for polymorphisms was performed by screening six individuals from F_1 for more than 200 microsatellite markers (Koevoets et al., 2012; Niehuis et al., 2011; van de Zande et al., 2014). A universal primer (CAGGACCAGGCTACCGTG) was added to the 5′ end of the forward primers following the method of Blacket et al. (2012). The seven microsatellite markers that showed a polymorphism and were distributed over the five chromosomes of *N. vitripennis* were used to determine genetic variation. Details of these seven microsatellite markers are listed in Table S1. Primer pairs that failed in amplification or that were monomorphic were discarded. The amplifications were performed using the GoTaq Green Master Mix (Cat No. M7123, Promega, USA) in a final volume of 15 μl. The polymerase chain reaction (PCR) reaction mixture contained three primers: 0.08 μl forward primer, 0.16 μl reverse primer, and 0.32 μl fluorescently labeled universal primer (6FAM, VIC, and NED sequencing dyes). PCR was performed for two min at 95°C, followed by 30 cycles of 95°C for 45 s, 55/60°C for 45 s, and 72°C for 25 s, with a final extension at 72°C for 5 min. PCR products were analyzed on an ABI 3730xl Genetic Analyzer (Applied Biosystems, USA) using the GeneScan 500 LIZ size standard (Applied Biosystems, USA) from DNA Fragment Analysis of Massachusetts General Hospital.

Genotyping was conducted using GENEMAPPER 4.0 (Applied Biosystems, USA). Population genetic statistics (allelic richness R, heterozygosity HE, fixation index Fst) were calculated using FSTAT 2.9.3 (https://www2.unil.ch/izea/softwares/fstat.html). Nei's standard genetic distance (Dst) (Nei, 1972) and Fst phylogenetic trees using the unweighted pair-group method with arithmetic mean (UPGMA) and neighbor-joining method are constructed by POPTREE2 (Takezaki et al., 2010). We examined population genetic structure using STRUCTURE 2.3.4 (Pritchard et al., 2000) based on the Bayesian clustering approach. We used the admixture models and correlated allele frequencies for the analyses. The clustering test was replicated 20 times with 200,000 Markov chain Monte Carlo Iterations following a burn-in of 100,000 iterations under each K value (from one to seven).

Bioluminescence Assay

Bacterial strains were cultured in flasks containing NB medium and 100 ppm atrazine at 30°C and 250 rpm for 18 h. The culture was centrifuged at 6000 rpm for 5 min, the supernatant was removed, and the resulting cell pellet was resuspended in the same volume of NB media, and centrifuged again at 6000 rpm for 3 min. The resulting cell pellet was resuspended in NB media to OD 620 = 0.002. To heat-killed bacteria, the strains were kept at 100°C for 1 h. NB medium (30 mg/l atrazine) was inoculated using 1% concentration of the inoculum and shaken at 250 rpm at 30°C ($\approx 4.0 \times 10^6$ *P. protegens* NVIT02 cells/mL, $\approx 9.6 \times 10^6$ *S. marcescens* NVIT01 cells/mL, $\approx 2 \times 10^5$ SM004 cells/mL). As a positive control, the *E. coli* strain SM004 was used, and isopropyl β-D-thiogalactoside was added to the media (to a final concentration of 2mM) to induce expression of atrazine metabolizing genes. Aliquots of the cultures were taken at 12, 21, and 24 h. All experiments were performed in triplicate. To assess the final atrazine concentration of the media, bioluminescence measurements were performed following the method described by Hua et al. (2015). The SM004 suspension was induced with 20 μl atrazine solution as collected above. Two hundred μl of the bacterial suspensions were transferred into a white 96-well microplate for bioluminescence measurement. Bioluminescence was recorded over 2 h with an acquisition time of one second per well at 30°C using a Synergy H1 reader (BioTek Instruments, Inc.).

LCMS Assay

Atrazine was analyzed by high-performance LCMS using a Shimadzu LC-20 liquid chromatograph equipped with an ACE C18 column (3 mm, 150 × 4.6 mm), a Shimadzu SPD-M20A diode array detector, and an Applied Biosystems SCIEX API 2000 triple quadrupole mass spectrometer (operating in positive electrospray ionization mode). Compounds were separated with a binary mobile phase flowing at 0.5 mL min^{-1} consisting of acidified water (0.1% formic acid, v/v; solvent A) and acidified acetonitrile (0.1% formic acid, v/v; solvent B). The gradient was as follows: 10% B (two min hold) ramped to a final mobile phase concentration of 100% B over 18 min (with a 5 min hold). Compounds that eluted from samples were characterized by retention time and, where applicable, characteristic UV-Vis chromophores (λ_{max}) and positively-charged ions. Under these conditions, the retention time of atrazine was 16.93 min. The concentrations of atrazine in samples were quantified by integrating peak areas compared to a purchased standard.

Identification of Atrazine-Degrading Bacterial Strains and Genes

Isolated bacterial strains were grown in Nutrition Broth liquid media, and DNA was extracted using DNeasy Blood & Tissue Kit (QIAGEN, Hilden, Germany). PCR was performed using either *16S* universal primers or atrazine gene primers (Table S1) and TaKaRa Ex Taq DNA Polymerase according to the manufacturer's instructions. Products were purified using Agencourt AMPure XP, quantified using the dsDNA HS Assay kit on the Qubit, and sequenced by Genewiz, Inc. (South Plainfield, NJ). Sequences were compared using BLAST against annotated sequences in GenBank.

To construct a phylogenetic tree, representative strains were selected that most closely related to the sequenced isolates using the *16S* rRNA gene information from the GenBank (https://www.ncbi.nlm.nih.gov/genbank/). *16S* rRNA sequences were aligned using Infernal, a stochastic context-free grammar-based aligner (Cole et al., 2014). PhyML 3.0 (Guindon et al., 2010) was used to build a Maximum Likelihood (ML) phylogenetic tree.

Bacterial Genome DNA Preparation, Sequencing, and Analysis

Bacterial strains were cultured in NB medium at 30°C, agitated at 250 rpm in flasks for 18 h and later centrifuged at 6000 rpm for five min. The resulting cell pellet was used for genome extraction using the DNeasy Blood & Tissue Kit (QIAGEN, Hilden, Germany) and plasmid DNA extraction using QIAGEN Plasmid Mini Kit (QIAGEN, Hilden, Germany). DNA was quantified using the dsDNA HS Assay kit on the Qubit 2.0 Fluorometer (Life Technologies, Waltham, USA). Genomic DNA was prepared using Nextera XT library prep kit

(Illumina) following the manufacturer's protocol. Library preparation was performed using a Microlab STAR automated liquid handling system (Hamilton) and libraries were sequenced on the Illumina HiSeq using a 250 bp paired end protocol at MicrobesNG (Birmingham, United Kingdom).

Following the same methods and parameters for trimming the reads, the quality assessment, assembling contigs, and genome annotation outlined in Wang and Brucker (2019). The draft genomes are summarized in Table S6.

Bacterial Feeding for Probiotic Assay

The adults were fed *S. marcescens* NVIT01 in sugar solution, *P. protegens* NVIT02 in sugar solution (OD 620 = 0.4, $\approx 8 \times 10^8$ *P. protegens* NVIT02 cells/mL, OD 620 = 0.084, $\approx 2 \times 10^9$ *S. marcescens* NVIT01 cells/mL) or sugar solution only. The bacterial preparation is same as described above for the bioluminescence assay. The median LC50 was measured for the next generation offsprings.

QUANTIFICATION AND STATISTICAL ANALYSIS

General

Data was considered statistically significant when $p < 0.05$, Log-rank test, Mann-Whitney U test, Student's t test, PERMANOVA test, as indicated in the figure, figure legend or experimental methods. Asterisks denote corresponding statistical significance *$p < 0.05$; **$p < 0.01$; ***$p < 0.001$. * indicates the resistance ratio calculated by 95%. CI does not include 1.0 using Polo Plus-PC software for LC50. *$p < 0.05$ for nRF and nMC tests for congruency. Data is presented as the mean ± SD, mean ± SE, LC50 ± 95%CI where appropriate from at least 3 independent biological replicates, unless stated otherwise in figures, figure labels or experimental methods. Statistical analysis was performed using GraphPad Prism 7 software or R, PERMANOVA test in QIIME2, as indicated.

Quantification of Gene Expression

For RNA-seq analysis, a gene with a fold change > 1.5 (upregulated) or < 0.67 (downregulated) and P value < 0.05, FDR < 0.05 was considered to be a differentially expressed gene.

Quantification of Protein Expression

A protein with a fold change > 1.2 (upregulated) or < 0.83 (downregulated) and P value < 0.05 (Student's t test) was considered to be differentially regulated.

Quantification of Phylogeny Congruency

We used TreeCmp 2.0 (https://eti.pg.edu.pl/treecmp/) to quantify the congruency analyses between host phylogeny and microbiota topology. we re-rooted host and microbiota phylogeny trees using FigTree v1.4.2 (http://tree.bio.ed.ac.uk/software/figtree/) and followed Brooks et al. (2016) to calculate statistics.

DATA AND CODE AVAILABILITY

All *de novo* nucleotide Sanger sequences in this study were deposited in GenBank under accession numbers MG426189-MG426190, MG592715-MG592717, MG660865-MG660870, MK312633-MK312640. The bacteria whole-genome shotgun data has been deposited at DDBJ/ENA/GenBank under the accession number PEGE00000000 for *S. marcescens* NVIT01 and no. PISQ00000000 for *P. protegens* NVIT02. The version described in this paper is the first version. The proteomics data has been deposited to the ProteomeXchange Consortium via the PRIDE (https://www.ebi.ac.uk/pride) with the dataset identifier PXD011964. The RNA-seq raw reads and the *16S* rRNA data have been deposited as project number PRJNA509675 in the Sequence Read Archive of the National Center for Biotechnology Information. Additional data associated with this paper has been deposited at Mendeley Data at https://dx.doi.org/10.17632/v3csd6wmh7.1. The code supporting the current study are available from the corresponding author on request.